Polymer Effect on Heterochiral Molecular Recognition in Molecular and Macromolecular Pairs of Liquid Crystals of (*R*)- and (*S*)-2-Chloro-4-methylpentyl 4′-[[8-(Vinyloxy)octyl]oxy]biphenyl-4-carboxylate Enantiomers

Virgil Percec* and Hiroji Oda

Department of Macromolecular Science, Case Western Reserve University, Cleveland, Ohio 44106

Received December 22, 1993; Revised Manuscript Received December 22, 1993•

ABSTRACT: (*R*)-2-Chloro-4-methylpentyl 4′-[[8-(vinyloxy)octyl]oxy]biphenyl-4-carboxylate ((*R*)-8) (*R* >95%) and (*S*)-2-chloro-4-methylpentyl 4′-[[8-(vinyloxy)octyl]oxy]biphenyl-4-carboxylate ((*S*)-8) (*S* >95%) enantiomers and their corresponding homopolymers and copolymers with well-defined molecular weight and narrow molecular weight distribution were synthesized and characterized. The phase behavior of the two enantiomeric polymers can be compared only by superimposing the dependence of their transition temperatures as a function of molecular weight. The phase behaviors of (*R*)-8 and poly[(*R*)-8] are identical to those of (*S*)-8 and poly[(*S*)-8] respectively. Both monomers display monotropic S_A and S_C* phases and a crystalline phase, while the corresponding polymers exhibit enantiotropic S_A, S_C*, and S_X (unidentified smectic) mesophases. Phase diagrams were investigated in detail in binary mixtures of (*R*)-8 with (*S*)-8, poly[(*R*)-8] with poly[(*S*)-8] and in binary copolymers of (*R*)-8 with (*S*)-8 as a function of the composition of the two enantiomeric structural units. In all these systems the two enantiomeric structural units derived from the two monomers are miscible within all their mesophases and over the entire range of composition. This is in contrast to the crystalline phase of the monomers whose phase diagram displays an eutectic composition. The S_A–I transition of the binary mixture of (*R*)-8 with (*S*)-8 is within 0.4 °C higher in the 50/50 mixture than the theoretical value expected for an ideal solution, demonstrating the presence of heterochiral molecular recognition between the two enantiomers in their S_A phase. Heterochiral recognition was not detected in the S_C* phase of any of the enantiomeric pairs investigated. In the polymer mixtures, the chiral recognition observed in the S_A phase of the monomer mixtures is enhanced with increasing the degree of polymerization (DP) up to about 10 to reach a positive deviation of 1.3 °C from the theoretical ideal value. However, polymer mixtures with DP higher than 14 showed smaller positive deviations of their S_A–I transitions than those of the corresponding monomer mixtures. These results indicate the existence of an optimum molecular weight for the manifestation of heterochiral recognition. In the copolymer system, no clear trend was observed with respect to any phase.

Introduction

Chiral molecular recognition has recently received increasing interest in various areas of chemistry.[1] Although a variety of topics are of interest in this field, the most notable series of quantitative studies performed in the last decade refer to the investigation of chiral molecular recognition in monolayers consisting of pairs of enantiomers[2] and diastereomers.[3] The influence of chirality is also of considerable interest in the field of molecular thermotropic liquid crystals. Since the discovery of ferroelectric properties in the chiral smectic C (S_C*) phase, this field has become extremely active.[4] In most cases, attention has been paid mainly to the electrooptic properties of chiral liquid crystals. There is a limited number of publications in which the influence of chirality on the phase behavior of low molar mass liquid crystals was investigated as a function of their optical purity.[1a,5-9] In a few cases, it has been observed that chiral recognition occurs specifically in layered liquid crystalline phases and as a consequence increases the phase transition temperatures of the racemic mixture by comparison to those of the pure enantiomers.[1a,5,7,8] However, the relationship between molecular structure and the mechanism responsible for the manifestation of heterochiral recognition is far from being elucidated.

We reported a series of experiments on the molecular engineering of side-chain liquid crystalline polymers by using a living cationic polymerization technique as a tool to generate well-defined polymers.[10,11] As part of our continuing efforts to elucidate the molecular–supramolecular structures–properties dependence by this technique, we have initiated a series of systematic investigations on chiral molecular recognition using well-defined polymers obtained by the living cationic polymerization. In the first publication on this topic, we reported the observation of heterochiral recognition in molecular and macromolecular pairs of diastereomeric liquid crystals based on (2*R*,3*S*)- and (2*S*,3*S*)-2-fluoro-3-methylpentyl 4′-[[11-(vinyloxy)undecanyl]oxy]biphenyl-4-carboxylate (**9**).[12] Heterochiral recognition was observed in the S_A but not in the S_C*, S_X, and crystalline phases of the monomer. Heterochiral recognition was not observed in polymer mixtures and in copolymers.[12]

The first goal of this paper is to describe the synthesis and the living cationic polymerization of (*R*)-2-chloro-4-methylpentyl 4′-[[8-(vinyloxy)octyl]oxy]biphenyl-4-carboxylate ((*R*)-8) and (*S*)-2-chloro-4-methylpentyl 4′-[[8-(vinyloxy)octyl]oxy]biphenyl-4-carboxylate ((*S*)-8) enantiomers. The second goal of this paper is to compare the mesomorphic behavior of these two enantiomeric structural units and to investigate the heterochiral recognition in binary mixtures of monomers and of polymers, as well as in copolymers. To our knowledge, this paper will report the first example of heterochiral molecular recognition

* To whom all correspondence should be addressed.
• Abstract published in *Advance ACS Abstracts*, July 1, 1994.

0024-9297/94/2227-4454$04.50/0

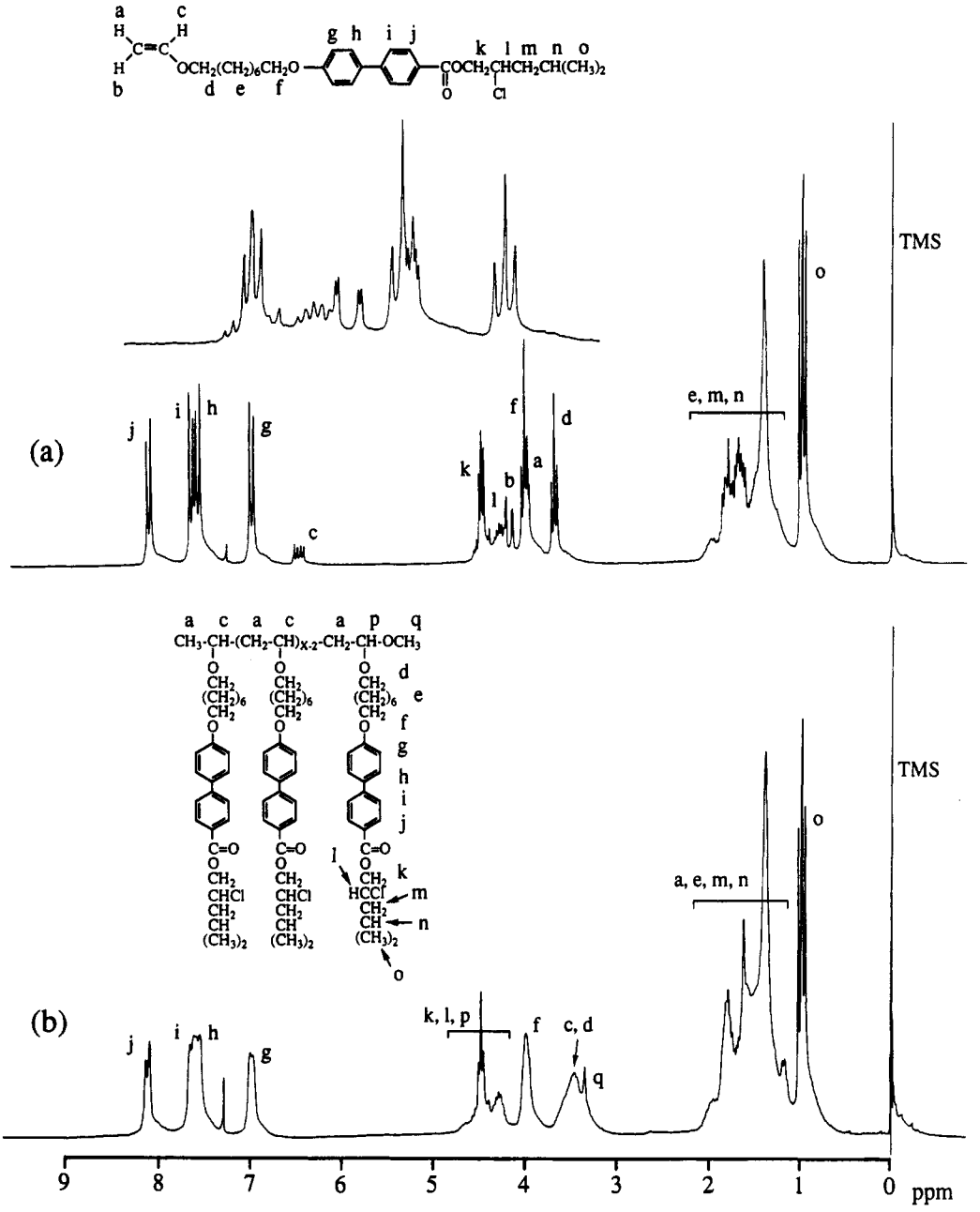

Figure 1. ^{1}H NMR spectra of monomer (*R*)-8 (a) and polymer poly[(*R*)-8] (DP = 5.7) (b).

present in both pairs of monomers and of side-chain liquid crystalline polymers.

Experimental Section

Materials. L-Leucine [(*S*)-(+)-2-amino-4-methylpentanoic acid, 99%, Aldrich], D-leucine [(*R*)-(−)-2-amino-4-methylpentanoic acid, 99%, Aldrich], and borane–tetrahydrofuran complex (BH_3·THF, 1.0 M solution in THF, Aldrich) were used as received.

Pyridine was heated overnight at 100 °C over KOH, distilled from KOH, and then stored over KOH. Dimethyl sulfoxide (DMSO) was heated overnight at 100 °C over CaH_2, distilled from CaH_2 under vacuum, and stored over molecular sieves (4 Å). THF was refluxed over $LiAlH_4$ for several days and distilled from $LiAlH_4$. Acetone was stored over anhydrous K_2CO_3 for several days, filtered, and distilled.

CH_2Cl_2 used as polymerization solvent was first washed with concentrated H_2SO_4 several times until the acid layer remained colorless, then washed with water, dried over $MgSO_4$, refluxed over CaH_2, and freshly distilled under argon before each use. Dimethyl sulfide [$(CH_3)_2S$] used in polymerizations (Aldrich, anhydrous, 99+%, packed under nitrogen in Sure/Seal bottle) was used as received. Trifluoromethanesulfonic acid (CF_3SO_3H) used as polymerization initiator (Aldrich, 98%) was distilled under vacuum.

All other materials were commercially available and were used as received.

Techniques

^{1}H NMR spectra were recorded on Varian XL-200 (200 MHz) spectrometer.

Relative molecular weights of polymers were determined by gel permeation chromatography (GPC). GPC analyses were carried out with a Perkin-Elmer Series 10LC instrument equipped with an LC-100 column oven and a Nelson Analytical 900 Series data station. Measurements were made by using a UV detector, THF as solvent (1 ml/min, 40 °C), a set of PL gel columns of 5×10^2 and 10^4 Å, and a calibration plot constructed with polystyrene standards.

A Perkin-Elmer PC Series DSC-7 differential scanning calorimeter was used to determine the thermal transition temperatures, which were reported as the maxima and

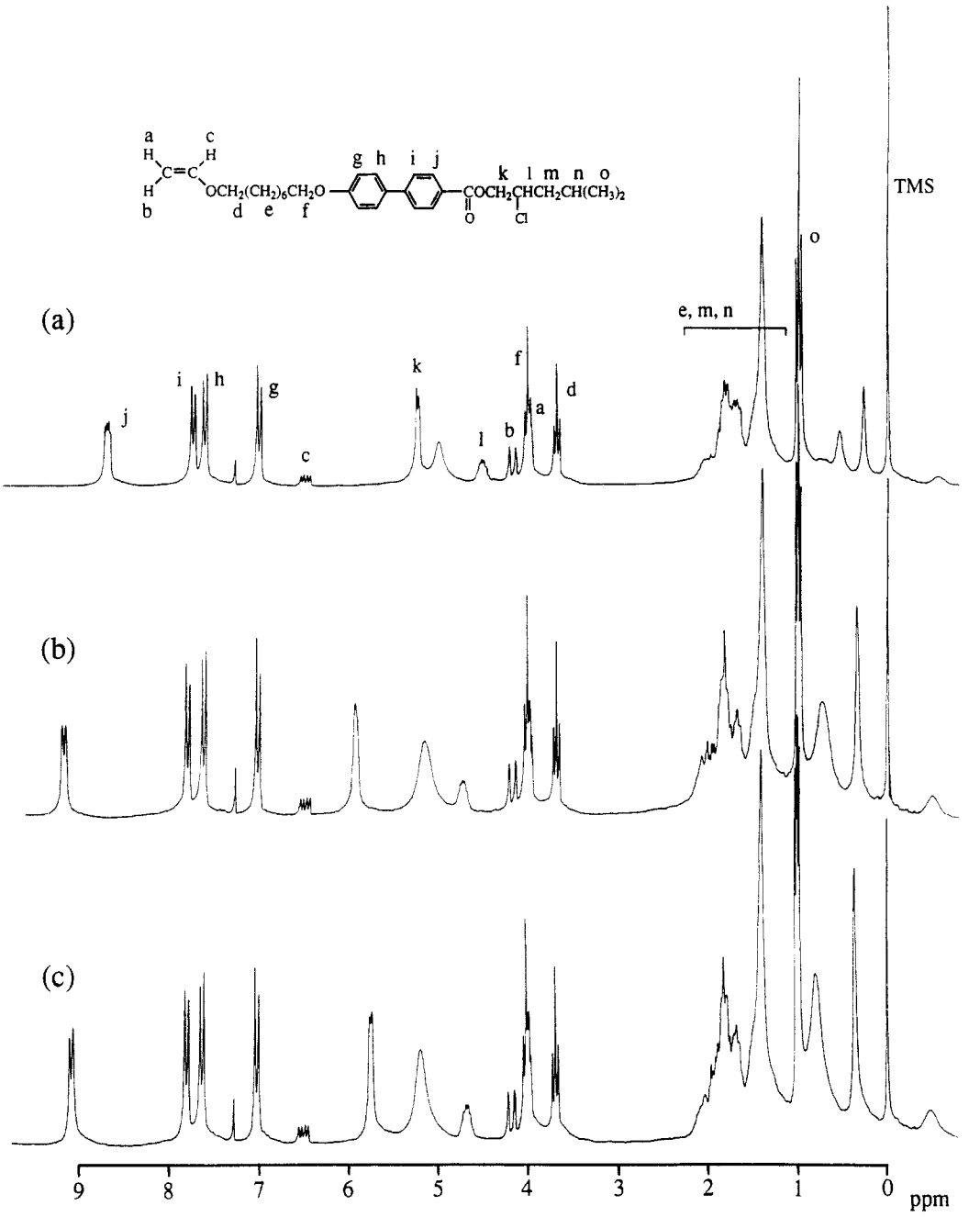

Figure 2. ^{1}H NMR spectra of monomer mixture and monomers with Eu(hfc)$_3$: (a) (*R*)-8/(*S*)-8 (50/50 mixture), (b) (*R*)-8, and (c) (*S*)-8.

minima of their endothermic or exothermic peaks, respectively. Heating and cooling rates were 20 °C/min for the analysis of the homopolymers and 10 °C/min for the analysis of the monomer and polymer mixtures and of copolymers.

A Carl-Zeiss optical polarizing microscope equipped with a Mettler FP-82 hot stage and a Mettler FP-80 central processor was used to observe the thermal transitions and to analyze the anisotropic textures.

Synthesis of Monomers. Monomers (*R*)-8 and (*S*)-8 were synthesized from D-(*R*)-leucine and L-(*S*)-leucine, respectively, according to the reaction pathway outlined in Scheme 1. The synthesis of compounds 5 and 7 was described previously.[11] This synthetic procedure will be described in detail only for monomer (*S*)-8.

(*S*)-2-Chloro-4-methylpentanoic Acid [(*S*)-2].[13] A solution of $NaNO_2$ (19.7 g, 0.286 mol) in water (50 mL) was added dropwise to a stirred, cooled (0 °C) mixture of

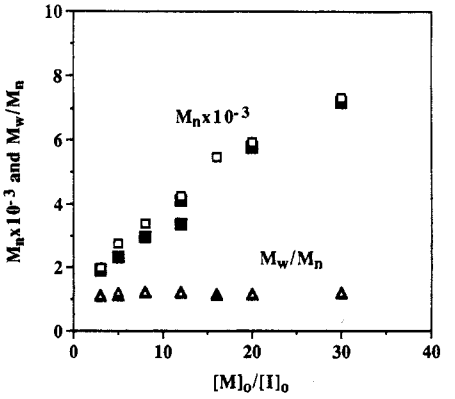

Figure 3. Dependence of the number average molecular weight (M_n) and polydispersity (M_w/M_n) of poly[(*R*)-8] (open symbols) and poly[(*S*)-8] (closed symbols) determined by GPC on the $[M]_o/[I]_o$ ratio.

L-leucine (25.0 g, 0.191 mol), concentrated HCl (125 mL) and water (125 mL) over 1.5 h. Stirring was continued overnight while the mixture was allowed to warm to room temperature. The product was extracted into diethyl ether four times and the combined ethereal extracts were dried over anhydrous $MgSO_4$. The solvent was evaporated and the remaining crude product was distilled under vacuum to yield a colorless liquid (18.4 g, 64.1%), bp 82–86 °C (2 mmHg). ^{1}H NMR ($CDCl_3$, TMS): δ 1.00 (m, 6H, $(CH_3)_2$-CH–), 1.88 (m, 3H, $(CH_3)_2CHCH_2$–), 4.36 (m, 1H, –CHCl–), 10.23 (bs, 1H, –COOH).

(*S*)-2-Chloro-4-methylpentanol [(*S*)-3]. A solution of BH_3·THF complex in THF (1.0 M, 62.5 mL, 62.5 mmol) was added dropwise to a stirred, cooled (0 °C) solution of (*S*)-2 (7.84 g, 52.1 mmol) in dry THF (150 mL) over 1 h under nitrogen atmosphere. The reaction mixture was allowed to warm to room temperature and stirring was continued for 2 h. Then the reaction mixture was cooled to 0 °C again and 7 mL of water followed by 150 mL of saturated K_2CO_3 solution was added. The product was extracted into diethyl ether twice, and the combined organic layers were dried over anhydrous $MgSO_4$. The solvent was evaporated, and the remaining crude product (6.43 g, 90.3%) was used for the synthesis of (*S*)-4 without further purification. ^{1}H NMR ($CDCl_3$, TMS): δ 0.92 (d, J = 6.5 Hz, 3H, $(CH_3)_2$CH–), 0.96 (d, J = 6.5 Hz, 3H, $(CH_3)_2$CH–), 1.39–1.58, 1.58–1.79 (m, 2H, $(CH_3)_2CHCH_2$–), 1.79–1.97 (m, 1H, $(CH_3)_2CHCH_2$–), 2.19 (bs, 1H, $-CH_2OH$), 3.57–3.89 (m, 2H, $-CH_2OH$), 4.11 (m, 1H, –CHCl–).

(*S*)-2-Chloro-4-methylpentyl Tosylate [(*S*)-4]. A solution of (*S*)-3 (6.43 g, 47.1 mmol, crude) in dry pyridine (20 mL) was added dropwise to a stirred, cooled (0 °C) solution of *p*-toluenesulfonyl chloride (13.5 g, 70.7 mmol) in dry pyridine (80 mL). The mixture was allowed to warm to room temperature and stirred overnight. The mixture was poured into water, and the product was extracted into diethyl ether twice. The combined ethereal extracts were washed with 10% HCl twice and dried over anhydrous $MgSO_4$. The solvent was evaporated and the remaining crude product was purified by column chromatography (silica gel; hexane–ethyl acetate 15:1) to give a colorless liquid (10.2 g, 74.5%), purity >99% (TLC). ^{1}H NMR ($CDCl_3$, TMS): δ 0.86 (d, J = 6.5 Hz, 3H, $(CH_3)_2$CH–), 0.92 (d, J = 6.5 Hz, 3H, $(CH_3)_2$CH–), 1.50–1.61 (m, 2H, $(CH_3)_2CHCH_2$–), 1.78–1.94 (m, 1H, $(CH_3)_2CH$–), 2.46 (s, 3H, $-PhCH_3$), 3.97–4.18 (m, 3H, $-CHClCH_2OSO_2$–), 7.37 (d, J = 8.2 Hz, 2ArH, ortho to $-CH_3$), 7.82 (d, J = 8.2 Hz, 2ArH, ortho to $-SO_2$–).

(*S*)-2-Chloro-4-methylpentyl 4′-Hydroxybiphenyl-4-carboxylate [(*S*)-6]. A mixture of (*S*)-4 (8.72 g, 30.0 mmol), 5 (7.57 g, 30.0 mmol), tetrabutylammonium hydrogen sulfate (TBAH, 1.50 g), and dry DMSO (100 mL) was stirred at 80 °C under nitrogen atmosphere for 20 h. The resulting clear yellow solution was poured into water. The product was extracted into diethyl ether twice, and the combined ethereal extracts were dried over anhydrous $MgSO_4$. The solvent was evaporated, and the remaining crude product was purified by column chromatography twice (silica gel; hexane–ethyl acetate 3:1) to give a white solid (7.00 g, 73.6%); purity >99% (TLC); mp 81.2 °C (DSC, 20 °C/min). ^{1}H NMR ($CDCl_3$, TMS): δ 0.96 (d, J = 6.6 Hz, 3H, $(CH_3)_2$CH–), 0.99 (d, J = 6.6 Hz, 3H, $(CH_3)_2$CH–), 1.52–1.87 (m, 2H, $(CH_3)_2CHCH_2$–), 1.87–2.11, (m, 1H, $(CH_3)_2CH$–), 4.19–4.59 (m, 3H, $-CHClCH_2$-OCO–), 5.28 (s, 1H, –PhOH), 6.95 (d, J = 8.7 Hz, 2ArH, ortho to –OH), 7.54 (d, J = 8.7 Hz, 2ArH, meta to –OH), 7.63 (d, J = 8.5 Hz, 2ArH, meta to –COO–), 8.12 (d, J = 8.5 Hz, 2ArH, ortho to –COO–).

Scheme 1. Synthesis of Monomers (*R*)- and (*S*)-8

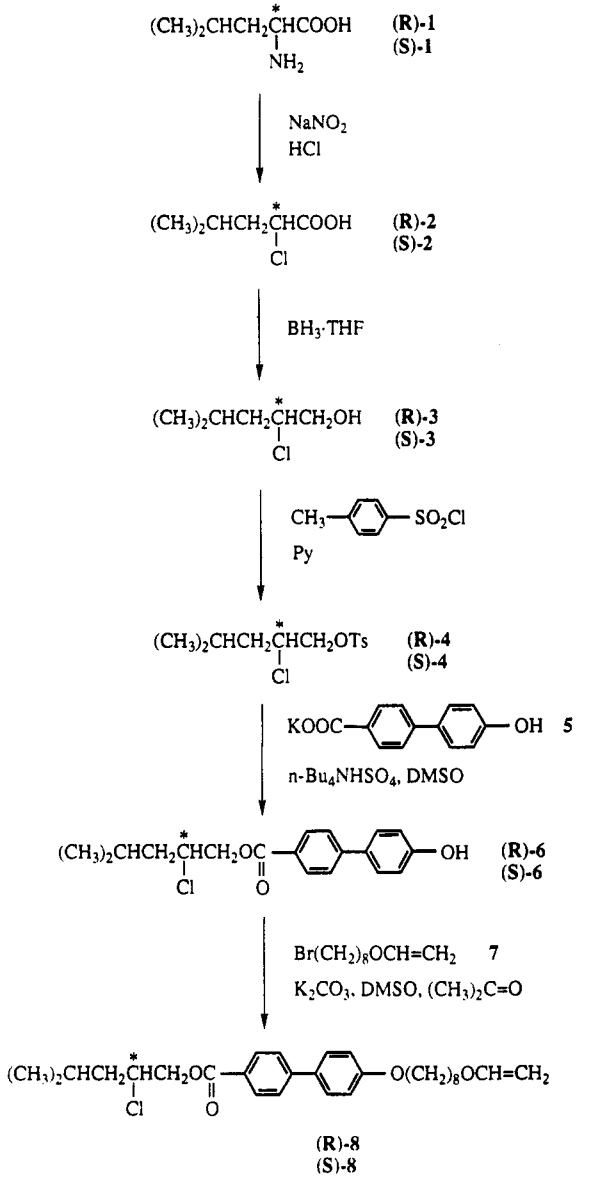

Scheme 2. Cationic Polymerization of (*R*)- and (*S*)-8

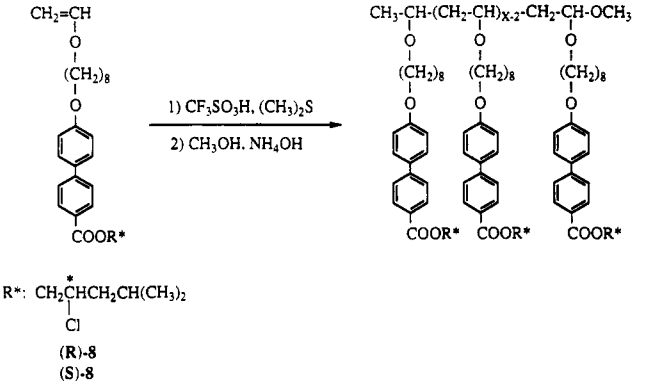

(*S*)-2-Chloro-4-methylpentyl 4′-[[8-(Vinyloxy)octyl]oxy]biphenyl-4-carboxylate [(*S*)-8]. A mixture of (*S*)-6 (3.50 g, 10.5 mmol), anhydrous K_2CO_3 (3.80 g, 27.5 mmol) and dry acetone (90 mL) was stirred at 60 °C under a nitrogen atmosphere for 2 h. To the resulting yellow solution was added a solution of 7 (2.59 g, 11.0 mmol) in dry DMSO (5.0 mL) and stirring was continued at 60 °C for 20 h. The mixture was poured into water, and the

Table 1. Cationic Polymerization of (*R*)-2-Chloro-4-Methylpentyl 4'-[[8-(Vinyloxy)octyl]oxy]biphenyl-4-carboxylate ((*R*)-8) and Characterization of the Resulting Polymers[a]

sample no.	$[M]_o/[I]_o$	polymer yield (%)	$M_n \times 10^{-3}$	M_w/M_n	DP	phase transitions (°C) and corresponding enthalpy chnages (kcal/mru)[b] heating	cooling
1	3	52.1	1.99	1.12	4.1	S_C*53.1 (0.34) S_A 56.0 (1.03) I S_C* 53.0 (0.32) S_A 56.3 (1.00) I	I 47.3 (-1.21) S_C*
2	5	78.6	2.76	1.14	5.7	S_C* 59.3 (0.31) S_A 62.2 (0.84) I S_C* 59.0 (0.32) S_A 62.1 (0.80) I	I 52.4 (-1.04) S_C*
						S_C* 64.6 (0.27) S_A 69.4 (0.82) I S_C* 64.2 (0.27) S_A 70.5 (0.81) I	I 60.4 (-0.97) S_C*
4	12	91.0	4.25	1.22	8.7	K 41.5 (0.58) S_C* 72.1 (0.27) S_A 77.1 (0.92) I S_X 35.1 (0.08) S_C* 71.1 (0.29) S_A 76.2 (0.82) I	I 66.1 (-1.12) S_C* 26.2 (-0.07) S_X
5	16	80.3	4.75	1.16	9.6	S_X 43.2 (0.07) S_C* 74.5 (0.33) S_A 78.8 (0.71) I S_X 41.5 (0.08) S_C* 74.2 (0.28) S_A 78.2 (0.72) I	I 68.1 (-1.04) S_C* 33.6 (-0.08) S_X
6	20	78.3	5.93	1.16	12.2	S_X 52.1 (0.11) S_C* 77.3 (0.30) S_A 81.7 (0.78) I S_X 50.8 (0.12) S_C* 76.9 (0.28) S_A 81.1 (0.77) I	I 71.4 (-1.06) S_C* 43.5 (-0.10) S_X
7	30	82.5	7.33	1.20	15.1	S_X 62.9 (0.16) S_C* 81.3 (0.28) S_A 85.9 (0.82) I S_X 61.7 (0.18) S_C* 80.5 (0.30) S_A 84.8 (0.75) I	I 75.0 (-1.03) S_C* 54.3 (-0.16) S_X

[a] Polymerization temperature, 0 °C; polymerization solvent, methylene chloride; $[M]_o$ = 0.224; $[Me_2S]_o/[I]_o$ = 10; polymerization time, 1 h. [b] Data on the first line are from first heating and cooling scans. Data on the second line are from second heating scan. Heating and cooling rates are 20 °C/min.

Table 2. Cationic Polymerization of (*S*)-2-Chloro-4-Methylpentyl 4'-[[8-(Vinyloxy)octyl]oxy]biphenyl-4-carboxylate ((*S*)-8) and Characterization of the Resulting Polymers[a]

sample no.	$[M]_o/[I]_o$	polymer yield (%)	$M_n \times 10^{-3}$	M_w/M_n	DP	phase transitions (°C) and corresponding enthalpy changes (kcal/mru)[b] heating	cooling
1	3	47.1	1.91	1.12	3.9	S_C* 52.3 (0.31) S_A 56.0 (0.90) I S_C* 52.1 (0.27) S_A 56.1 (0.89) I	I 47.7 (-1.06) S_C*
2	5	75.7	2.32	1.23	4.8	S_C* 56.7 (*c*) S_A 59.5 (1.13) I S_C* 55.8 (0.32) S_A 59.2 (0.77) I	I 49.6 (-1.02) S_C*
3	8	82.8	2.97	1.23	6.1	S_C* 63.0 (0.30) S_A 66.9 (0.77) I S_C* 62.6 (0.27) S_A 67.0 (0.80) I	I 57.4 (-1.01) S_C*
4	12	83.2	3.38	1.21	6.9	K 42.0 (0.16) S_C* 68.1 (0.34) S_A 72.0 (0.98) I S_X 18.6 (0.08) S_C* 67.1 (0.34) S_A 71.3 (0.92) I	I 61.4 (-1.21) S_C*
5	12	89.8	4.12	1.19	8.5	K 42.4 (0.62) S_C* 72.0 (0.29) S_A 77.0 (0.90) I S_X 34.2 (0.07) S_C* 71.5 (0.28) S_A 76.2 (0.80) I	I 66.1 (-1.05) S_C* 26.1 (-0.07) S_X
6	20	70.8	5.77	1.16	11.8	S_X 51.1 (0.13) S_C* 76.9 (0.37) S_A 81.3 (0.72) I S_X 49.2 (0.13) S_C* 76.1 (0.34) S_A 80.3 (0.73) I	I 70.9 (-1.03) S_C* 41.5 (-0.10) S_X
7	30	81.1	7.20	1.20	14.8	S_X 60.6 (0.17) S_C* 80.0 (0.31) S_A 84.5 (0.78) I S_X 58.6 (0.16) S_C* 78.9 (0.28) S_A 83.1 (0.77) I	I 73.4 (-1.06) S_C* 51.2 (-0.14) S_X

[a] Polymerization temperature. 0 °C; polymerization solvent, methylene chloride; $[M]_o$ = 0.224; $[Me_2S]_o/[I]_o$ = 10; polymerization time, 1 h. [b] Data on the first line are from first heating and cooling scans. Data on the second line are from second heating scan. Heating and cooling rates are 20 °C/min. [c] Overlapped peak.

Scheme 3. Cationic Copolymerization of (*S*)-8 with (2*S*,3*S*)-9

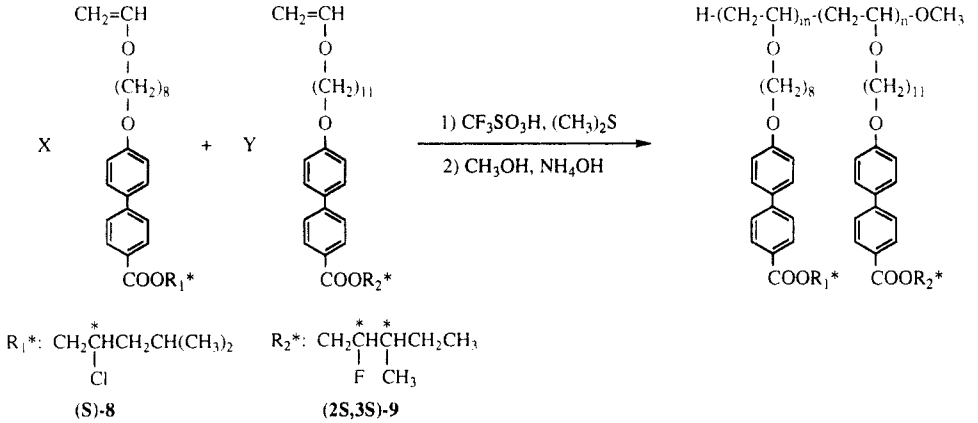

product was extracted into diethyl ether twice. The combined ethereal extracts were dried over anhydrous $MgSO_4$. The solvent was evaporated, and the remaining crude product was purified by column chromatography twice (silica gel; hexane–ethyl acetate 20:1) to yield a white solid (3.20 g, 62.6%), purity >99% (TLC). The thermal transition temperatures are given in Table 4. ^1H NMR ($CDCl_3$, TMS): δ 0.96 (d, J = 6.6 Hz, 3H, $(CH_3)_2CH$–), 0.99 (d, J = 6.6 Hz, 3H, $(CH_3)_2CH$–), 1.18–2.06 (m, 15H, $(CH_3)_2CHCH_2$–, CH_2=CHOCH$_2$$(CH_2)_6CH_2O$–), 3.68 (t, J = 6.5 Hz, 2H, CH_2=CHOCH_2–), 3.98 (dd, J = 6.8, 1.8 Hz, 1H, CH_2=CHO– trans), 4.01 (t, J = 6.5 Hz, 2H, –CH_2–OPh–), 4.18 (dd, J = 14.4, 1.8 Hz, 1H, CH_2=CHO– cis), 4.22–4.57 (m, 3H, –CHClCH_2OCO–), 6.48 (dd, J = 14.4, 6.8 Hz, 1H, CH_2=CHO–), 6.99 (d, J = 8.7 Hz, 2ArH, ortho to –$(CH_2)_8O$–), 7.57 (d, J = 8.7 Hz, 2ArH, meta to –$(CH_2)_8O$–), 7.65 (d, J = 8.3 Hz, 2ArH, meta to –COO–), 8.11 (d, J = 8.3 Hz, 2ArH, ortho to –COO–).

Cationic Polymerization. Polymerizations and copolymerizations were carried out in a three-necked round-bottom flask equipped with a Teflon stopcock and rubber septa under argon atmosphere at 0 °C for 1 h. All glassware

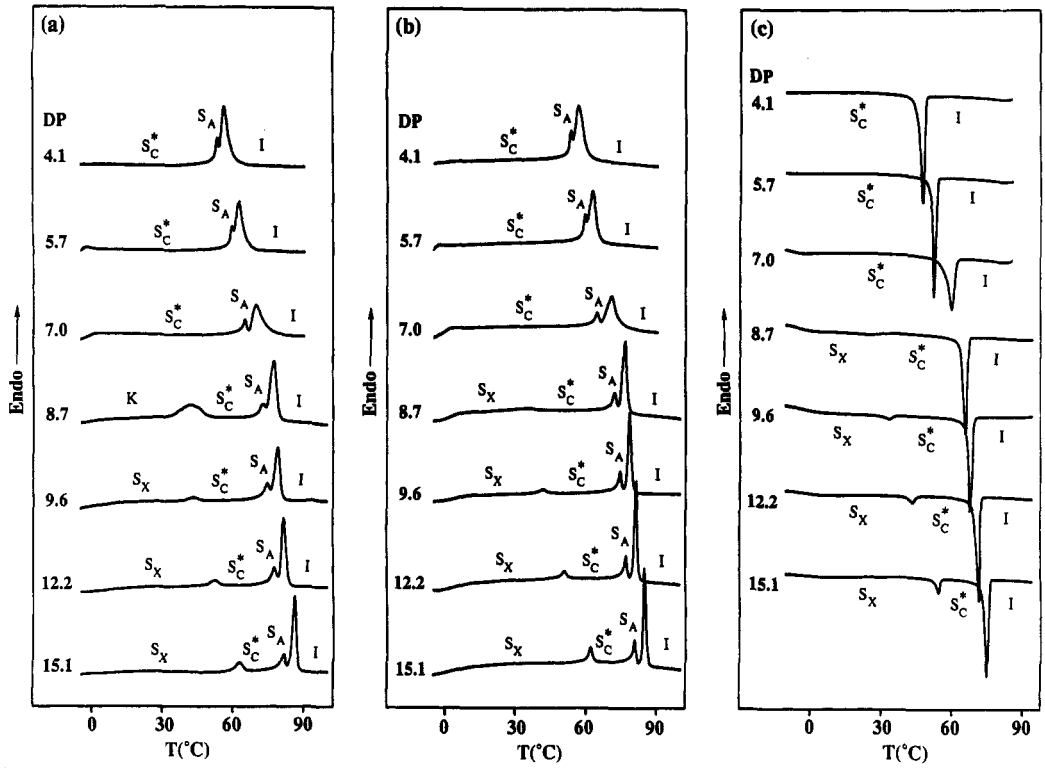

Figure 4. DSC thermograms (20 °C/min) of poly[(*R*)-8] with different DP: (a) first heating scans; (b) second heating scans; (c) first cooling scans.

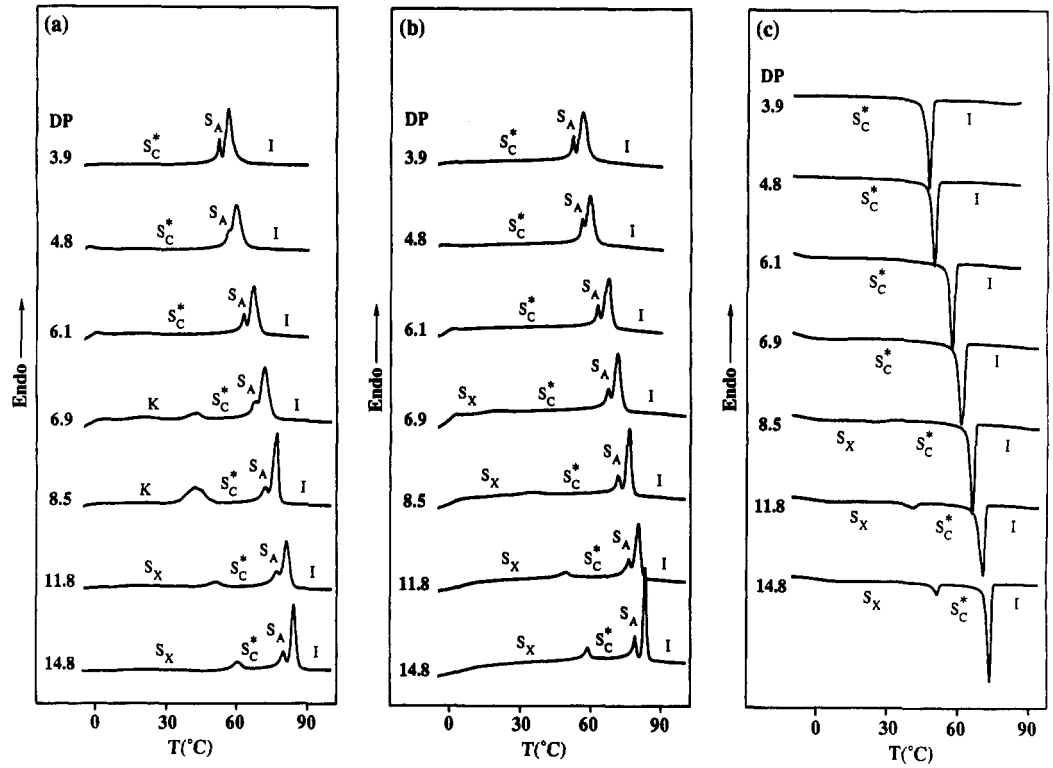

Figure 5. DSC thermograms (20 °C/min) of poly[(*S*)-8] with different DP: (a) first heating scans; (b) second heating scans; (c) first cooling scans.

was dried overnight at 140 °C. The monomer was further dried under vacuum overnight in the polymerization flask. After the flask was filled with argon, freshly distilled dry methylene chloride was added via a syringe and the solution was cooled to 0 °C. Dimethyl sulfide and trifluoromethanesulfonic acid were then added carefully via a syringe. The monomer concentration was about 0.224 M and the dimethyl sulfide concentration was 10 times larger than that of trifluoromethanesulfonic acid. The polymer molecular weight was controlled by the monomer/initiator ($[M]_o/[I]_o$) ratio. After quenching the polymerization with a mixture of NH_4OH and methanol (1:2), the reaction mixture was poured into methanol to give a white precipitate. The obtained polymer was purified by reprecipitation by pouring its chloroform solution into methanol and dried under vacuum.

Results and Discussion

Determination of the Optical Purities of Monomers (*R*)- and (*S*)-8. The synthesis of the two enantiomeric

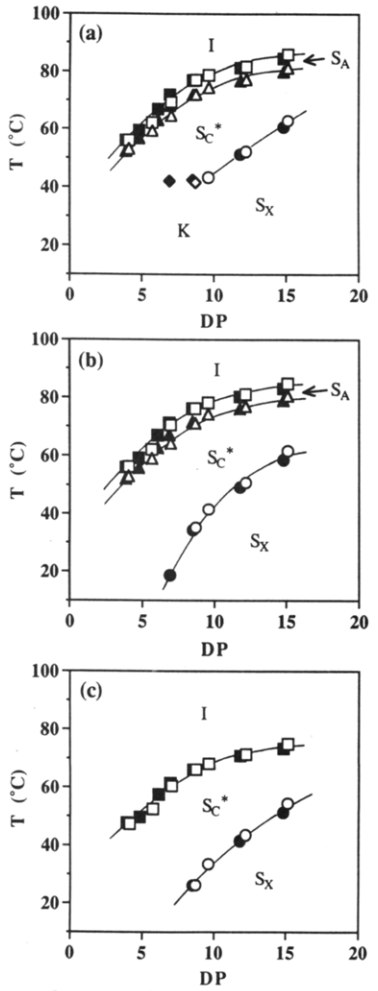

Figure 6. Dependence of phase transition temperatures on the degree of polymerization of poly[(***R***)-8] (open) and poly[(***S***)-8] (closed): (a) data from the first heating scans, (b) data from the second heating scans, and (c) data from the first cooling scans.

Figure 7. A representative optical polarized micrograph of the S_A mesophase displayed by poly[(***S***)-8] (DP = 11.8) upon heating to 78 °C (100×).

monomers (***R***)- and (***S***)-8 is outlined in Scheme 1. Monomers (***R***)-8 and (***S***)-8 were synthesized from D-(*R*)-leucine and L-(*S*)-leucine, respectively, in the same manner. The amino groups of D-(*R*)- and L-(*S*)-leucine were substituted with a chlorine atom via a diazonium salt by using $NaNO_2$ in 6 N HCl. Since this reaction proceeds with the retention of configuration at the chiral center, the original configurations of D-(*R*)- and L-(*S*)-leucine are maintained throughout the entire steps of the synthesis. The reduction of the carboxyl groups of compounds (***R***)- and (***S***)-2 was carried out with a BH_3·THF complex without

Table 3. Cationic Copolymerization of (*S*)-8 with (2*S*,3*S*)-9 and Characterization of the Resulting Polymers[a]

[(*S*)-8]/[(2*S*,3*S*)-9]	polymer yield (%)	$M_n \times 10^{-3}$	M_w/M_n	DP	phase transitions (°C) and corresponding enthalpy changes (kcal/mru)[b]	
					heating	cooling
0/100	74.0	5.78	1.10	11.3	K 53.0 (c) S_X 57.7 (1.39) S_C^* 92.4 (0.04) S_A 120.9 (1.17) I	I 111.7 (−1.17) S_A 85.6 (−0.04) S_C^* 48.2 (−0.88) S_X
10/90	79.9	5.37	1.23	10.5	S_X 57.2 (1.02) S_C^* 92.1 (0.03) S_A 120.3 (0.17) I K 50.4 (1.59) S_C^* 81.4 (0.03) S_A 116.5 (1.31) I S_X 49.2 (1.06) S_C^* 81.7 (0.04) S_A 116.4 (1.35) I	I 107.3 (−1.28) S_A 74.6 (−0.04) S_C^* 39.8 (−0.91) S_X
25/75	73.8	5.63	1.17	11.1	K 42.1 (1.46) S_C^* 70.8 (0.04) S_A 111.0 (1.28) I S_X 34.8 (0.86) S_C^* 70.6 (0.04) S_A 110.5 (1.26) I	I 101.4 (−1.21) S_A 63.7 (−0.03) S_C^* 25.7 (−0.71) S_X
40/60	67.9	5.57	1.21	11.1	K 38.5 (1.27) S_C^* 65.9 (0.04) S_A 106.5 (1.14) I S_X 31.2 (0.79) S_C^* 65.1 (0.05) S_A 106.3 (1.13) I	I 96.3 (−1.10) S_A 58.0 (−0.05) S_C^* 21.7 (−0.67) S_X
60/40	54.1	5.94	1.17	11.9	S_X 21.5(c) K 38.9 (0.58) S_C^* 63.9 (0.11) S_A 94.2 (0.94) I S_X 21.5 (0.52) S_C^* 63.4 (0.10) S_A 93.7 (0.95) I	I 84.2 (−0.92) S_A 57.0 (−0.10) S_C^* 11.3 (−0.43) S_X
75/25	81.4	5.94	1.21	12.0	S_X 33.6 (0.07) S_C^* 69.4 (0.15) S_A 89.7 (0.81) I S_X 31.3 (0.06) S_C^* 68.7 (0.17) S_A 89.2 (0.83) I	I 79.7 (−0.79) S_A 62.1 (−0.14) S_C^* 22.4 (−0.06) S_X
90/10	69.8	5.95	1.18	12.1	S_X 34.9 (0.06) S_C^* 70.1 (0.18) S_A 81.8 (0.73) I S_X 33.1 (0.06) S_C^* 69.8 (0.20) S_A 81.7 (0.72) I	I 72.1 (−0.69) S_A 63.2 (−0.17) S_C^* 23.9 (−0.05) S_X
100/0	70.8	5.77	1.16	11.8	S_X 51.1 (0.13) S_C^* 76.9 (0.37) S_A 81.3 (0.72) I S_X 49.2 (0.13) S_C^* 76.1 (0.34) S_A 80.3 (0.73) I	I 70.9 (−1.03) S_C^* 41.5 (−0.10) S_X

[a] Polymerization temperature, 0 °C; polymerization solvent, methylene chloride; $[M]_o = [(S)\text{-8}] + [(2S,3S)\text{-9}] = 0.224$; $[M]_o/[I]_o = 20$; $[Me_2S]_o/[I]_o = 10$; polymerization time, 1 h. [b] Heating and cooling rates are 20 °C/min. Data on the first line are from first heating and cooling scans. Data on the second line are from second heating scan. [c] Overlapped peak.

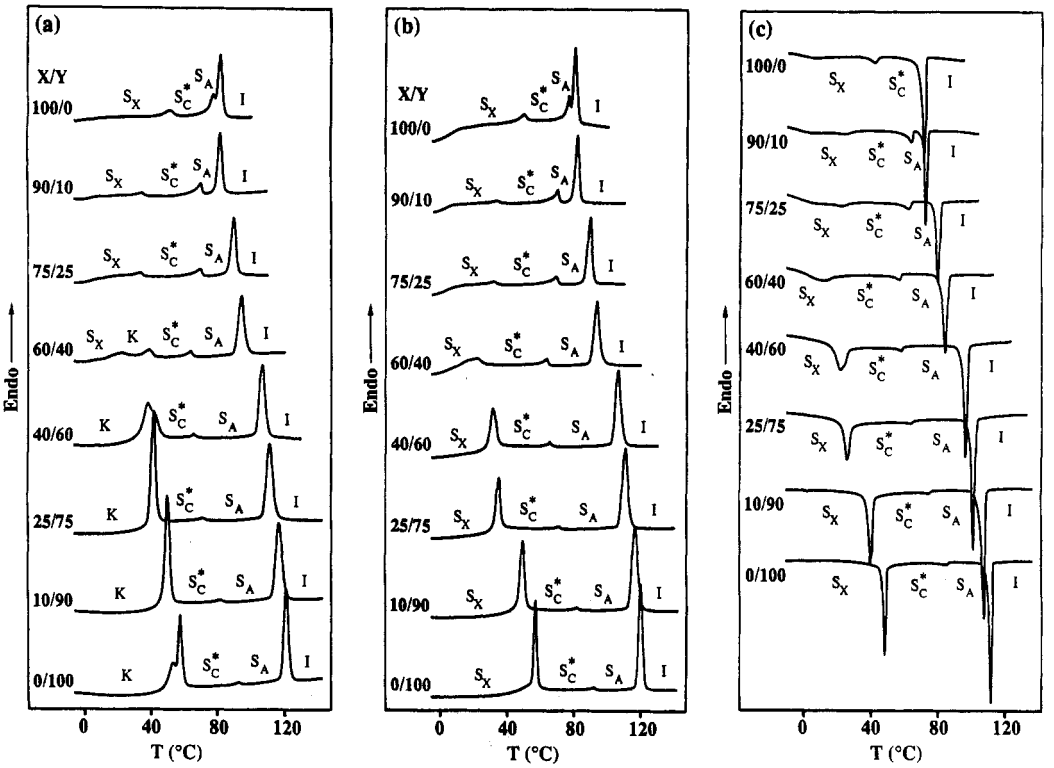

Figure 8. DSC thermograms (20 °C/min) of poly[[(*S*)-8]-*co*-[(2*S*,3*S*)-9]]*X*/*Y* with different compositions: (a) first heating scans, (b) second heating scans, and (c) first cooling scans.

Table 4. Characterization of the Binary Mixtures of Monomers (*R*)-8 with (*S*)-8

(*R*)-8/(*S*)-8 (mol)/(mol)	phase transitions (°C) and corresponding enthalpy changes (kcal/mol)[a]	
	heating	cooling
0/100	K 52.8 (11.80) I K 38.6 (3.10) K 40.1 (−1.50) K 49.5 (8.06) I	I 29.7 (−1.05) S_A 17.4 (−0.05) S_C^* 7.9 (−5.52) K
19.8/80.2	K 48.0 (11.40) I K 45.4 (10.73) I	I 30.2 (−1.03) S_A 17.5 (−0.05) S_C^* −4.8 (−5.60) K
39.0/61.0	K 49.4 (11.27) I K 48.3 (10.79) I	I 30.2 (−1.03) S_A 17.3 (−0.06) S_C^* −6.4 (−4.87) K
44.8/55.2	K 50.1 (11.49) I K 48.8 (11.06) I	I 30.3 (−1.05) S_A 17.2 (−0.06) S_C^* −6.6 (−4.99) K
49.9/50.1	K 50.2 (12.05) I K 42.5 (0.37) K 48.4 (10.93) I	I 30.2 (−1.10) S_A 16.9 (−0.07) S_C^* −6.6 (−5.35) K
55.0/45.0	K 49.5 (11.78) I K 48.6 (11.41) I	I 30.2 (−1.07) S_A 16.9 (−0.07) S_C^* −6.7 (−5.06) K
59.4/40.6	K 49.4 (11.22) I K 48.5 (11.12) I	I 30.2 (−1.06) S_A 16.9 (−0.07) S_C^* −6.7 (−5.13) K
80.0/20.0	K 48.2 (11.45) I	I 30.1 (−1.06) S_A 17.3 (−0.05) S_C^* −5.3 (−5.67) K
100/0	K 51.4 (−11.76) I K 38.6 (3.96) K 39.9 (−3.78) K 49.0 (9.14) I	I 29.9 (−1.04) S_A 17.4 (−0.06) S_C^* 6.7 (−5.86) K

[a] Data on the first line are from first heating and cooling scans. Data on the second line are from second heating scan. Heating and cooling rates are 10 °C/min.

affecting the chlorine atom of the chiral center. Reduction experiments with $LiAlH_4$ showed that it reduced the chlorine atom, resulting in the partial loss of the chiral center.

The optical purities of monomers (*R*)- and (*S*)-8 and of the corresponding polymers poly[(*R*)-8] and poly[(*S*)-8] were investigated by the NMR chiral shift reagent technique described by Goodby et al.[7b,14] The chiral shift reagent used in this study was tris[3-(heptafluoropropylhydroxymethylene)-(+)-camphorato] europium(III) derivative [$Eu(hfc)_3$]. Figure 1 presents the ^1H NMR spectra of monomer (*R*)-8 and polymer poly[(*R*)-8] (DP = 5.7) both without $Eu(hfc)_3$. Figure 2a presents the ^1H NMR spectrum of the 50/50 mixture between (*R*)- and (*S*)-8 with $Eu(hfc)_3$ [(*R*)-8 5 mg, (*S*)-8 5 mg, and $Eu(hfc)_3$ 10 mg]. The ^1H NMR spectra of pure (*R*)- and (*S*)-8 with $Eu(hfc)_3$ [monomer 10 mg and $Eu(hfc)_3$ 10 mg] are presented in Figure 2, parts b and c, respectively. As shown in Figure 2, the doublet associated with the aromatic proton j which is adjacent to the chiral center is split in the 50/50 mixture of the monomers, while the corresponding peaks remained unchanged in pure (*R*)- and (*S*)-8 except that they were shifted downfield. When the amount of the shift reagent was increased, a broadening of the peaks was observed before the complete separation of the two doublets was achieved and therefore, it was difficult to calculate the optical purities of both monomers precisely. However, judging from Figure 2, parts b and c, it seems that no racemization has occurred throughout the synthesis of the monomers and their optical purities are expected to be higher than 95%. The same technique was also applied to polymers. The polymers showed broadened peaks even in the absence of the shift reagent (Figure 1b) and this made the separation of the peaks impossible. However, it is believed that the chiral center of the

Table 5. Characterization of the Binary Mixtures of Poly[(*R*)-8] (DP = 5.7, M_w/M_n = 1.14) with Poly[(*S*)-8] (DP = 6.1, M_w/M_n = 1.23) (Polymer Mixture I)

poly[(*R*)-8]/poly[(*S*)-8] (mol)/(mol)	phase transitions (°C) and corresponding enthalpy changes (kcal/mru)[a]	
	heating	cooling
0/100	S_C^* 59.6 (0.19) S_A 64.1 (0.75) I S_C^* 59.2 (0.27) S_A 64.1 (0.77) I	I 57.6 (-1.02) S_A 56.3 (*b*) S_C^*
10.8/89.2	S_C^* 58.7 (0.19) S_A 63.3 (0.73) I S_C^* 58.7 (0.25) S_A 63.8 (0.78) I	I 57.4 (-0.98) S_A 55.4 (*b*) S_C^*
20.0/80.0	S_C^* 58.1 (0.20) S_A 62.6 (0.79) I S_C^* 58.0 (0.26) S_A 63.1 (0.83) I	I 57.0 (-1.06) S_A 54.8 (*b*) S_C^*
50.2/49.8	S_C^* 56.8 (0.21) S_A 61.2 (0.71) I S_C^* 56.4 (0.29) S_A 61.4 (0.80) I	I 55.3 (-1.03) S_C^*
59.3/40.7	S_C^* 56.8 (0.20) S_A 61.2 (0.81) I S_C^* 56.7 (0.28) S_A 61.8 (0.82) I	I 55.4 (-1.07) S_A 53.8 (*b*) S_C^*
80.7/19.3	S_C^* 56.0 (0.19) S_A 60.0 (0.83) I S_C^* 56.0 (0.29) S_A 60.6 (0.94) I	I 54.3 (-1.17) S_C^*
100/0	S_C^* 55.6 (0.20) S_A 59.1 (0.80) I S_C^* 55.4 (0.30) S_A 59.2 (0.85) I	I 52.9 (-1.06) S_C^*

[a] Data on the first line are from first heating and cooling scans. Data on the second line are from second heating scan. Heating and cooling rates are 10 °C/min. [b] Overlapped peak.

Table 6. Characterization of the Binary Mixtures of Poly[(*R*)-8] (DP = 6.7, M_w/M_n = 1.23) with Poly[(*S*)-8] (DP = 6.9, M_w/M_n = 1.21) (Polymer Mixture II)

poly[(*R*)-8]/poly[(*S*)-8] (mol)/(mol)	phase transitions (°C) and corresponding enthalpy changes (kcal/mru)[a]	
	heating	cooling
0/100	K 41.6 (0.38) S_C^* 63.9 (0.25) S_A 68.8 (0.78) I S_X 15.5 (0.05) S_C^* 63.6 (0.25) S_A 68.4 (0.74) I	I 61.8 (-0.98) S_C^*
21.4/78.6	S_X 14.0 (0.06) S_C^* 62.7 (0.25) S_A 67.2 (0.76) I S_X 12.4 (0.03) S_C^* 62.5 (0.24) S_A 67.7 (0.75) I	I 61.3 (-0.99) S_A 59.1 (*b*) S_C^*
39.1/60.9	S_C^* 62.0 (0.23) S_A 66.9 (0.76) I S_X 11.2 (0.02) S_C^* 61.7 (0.25) S_A 67.3 (0.76) I	I 61.1 (-1.00) S_A 58.5 (*b*) S_C^*
45.6/54.4	S_X 11.2 (0.01) S_C^* 61.6 (0.25) S_A 66.6 (0.76) I S_X 11.5 (0.03) S_C^* 61.5 (0.29) S_A 67.2 (0.78) I	I 61.2 (-1.00) S_A 58.3 (*b*) S_C^*
50.1/49.9	S_C^* 61.5 (0.28) S_A 66.4 (0.80) I S_X 10.2 (0.02) S_C^* 61.5 (0.22) S_A 67.1 (0.76) I	I 61.2 (-0.95) S_A 58.2 (*b*) S_C^*
54.9/45.1	S_X 10.1 (0.04) S_C^* 61.5 (0.24) S_A 66.2 (0.75) I S_X 10.2 (0.03) S_C^* 61.3 (0.25) S_A 67.1 (0.77) I	I 60.8 (-0.97) S_A 57.9 (*b*) S_C^*
59.0/41.0	S_X 11.1 (0.02) S_C^* 61.8 (0.25) S_A 66.7 (0.80) I S_X 10.7 (0.02) S_C^* 61.6 (0.23) S_A 67.2 (0.76) I	I 61.1 (-0.95) S_A 58.2 (*b*) S_C^*
88.4/11.6	S_C^* 60.1 (0.24) S_A 64.9 (0.78) I S_C^* 59.9 (0.26) S_A 65.4 (0.78) I	I 59.6 (-1.00) S_A 56.9 (*b*) S_C^*
100/0	S_C^* 59.6 (0.22) S_A 64.2 (0.74) I S_C^* 59.5 (0.26) S_A 64.8 (0.77) I	I 58.8 (-0.98) S_A 56.4 (*b*) S_C^*

[a] Data on the first line are from first heating and colling scans. Data on the second line are from second heating scan. Heating and cooling rates are 10 °C/min. [b] Overlapped peak.

Table 7. Characterization of the Binary Mixtures of Poly[(*R*)-8] (DP = 9.6, M_w/M_n = 1.16) with Poly[(*S*)-8] (DP = 10.1, M_w/M_n = 1.16) (Polymer Mixture III)

poly[(*R*)-8]/poly[(*S*)-8] (mol)/(mol)	phase transitions (°C) and corresponding enthalpy changes (kcal/mru)[a]	
	heating	cooling
0/100	S_X 42.2 (0.21) K 45.5 (*b*) S_C^* 71.1 (0.17) S_A 75.3 (0.80) I S_X 40.6 (0.08) S_C^* 70.7 (0.28) S_A 75.2 (0.71) I	I 69.0 (-1.00) S_A 67.3 (*b*) S_C^* 35.9 (-0.07) S_X
27.1/72.9	S_X 40.1 (0.05) K 44.8 (0.02) S_C^* 70.7 (0.21) S_A 75.0 (0.76) I S_X 39.4 (0.08) S_C^* 70.7 (0.25) S_A 75.4 (0.78) I	I 69.7 (-0.77) S_A 67.5 (-0.27) S_C^* 35.2 (-0.08) S_X
34.4/65.6	S_X 40.2 (0.06) S_C^* 70.7 (0.21) S_A 75.3 (0.76) I S_X 39.4 (0.08) S_C^* 70.8 (0.29) S_A 75.6 (0.75) I	I 69.9 (-0.74) S_A 67.5 (-0.26) S_C^* 35.7 (-0.08) S_X
44.3/55.7	S_X 39.9 (0.04) S_C^* 70.6 (0.20) S_A 75.1 (0.74) I S_X 39.0 (0.08) S_C^* 70.6 (0.26) S_A 75.5 (0.75) I	I 69.7 (-0.73) S_A 67.4 (-0.25) S_C^* 35.3 (-0.10) S_X
47.1/52.9	S_X 40.0 (0.06) S_C^* 70.8 (0.23) S_A 75.3 (0.75) I S_X 39.4 (0.09) S_C^* 70.8 (0.23) S_A 75.7 (0.80) I	I 70.2 (-0.75) S_A 67.6 (-0.26) S_C^* 36.0 (-0.07) S_X
49.9/50.1	S_X 39.4 (0.05) S_C^* 70.8 (0.20) S_A 75.4 (0.81) I S_X 39.4 (0.09) S_C^* 70.7 (0.29) S_A 75.6 (0.77) I	I 69.7 (-0.76) S_A 67.3 (-0.28) S_C^* 35.3 (-0.08) S_X
55.5/44.5	S_X 39.8 (0.05) S_C^* 70.9 (0.19) S_A 75.4 (0.72) I S_X 39.4 (0.08) S_C^* 70.8 (0.27) S_A 75.8 (0.74) I	I 69.9 (-0.74) S_A 67.6 (-0.27) S_C^* 35.9 (-0.08) S_X
74.9/25.1	S_X 39.4 (*b*) K 44.3 (0.10) S_C^* 70.8 (0.23) S_A 75.2 (0.73) I S_X 38.6 (0.08) S_C^* 70.7 (0.28) S_A 75.6 (0.74) I	I 69.6 (-0.71) S_A 67.4 (-0.26) S_C^* 34.6 (-0.06) S_X
100/0	K 43.8 (0.37) S_C^* 70.8 (0.26) S_A 75.0 (0.73) I S_X 39.0 (0.08) S_C^* 70.7 (0.29) S_A 75.2 (0.75) I	I 68.8 (-1.00) S_A 67.3 (*b*) S_C^* 34.0 (-0.07) S_X

[a] Data on the first line are from first heating and cooling scans. Data on the second line are from second heating scan. Heating and cooling rates are 10 °C/min. [b] Overlapped peak.

monomers is insensitive to the cationic polymerization condition and that the original optical purities of the monomers remain unchanged during this polymerization process. This was the case in previous examples of cationic polymerization of similar chiral monomers with the same initiating system.

Table 8. Characterization of the Binary Mixtures of Poly[(*R*)-8] (DP = 15.1, M_w/M_n = 1.20) with Poly[(*S*)-8] (DP = 14.3, M_w/M_n = 1.19) (Polymer Mixture IV)

poly[(*R*)-8]/poly[(*S*)-8] (mol)/(mol)	phase transitions (°C) and corresponding enthalpy changes (kcal/mru)[a]	
	heating	cooling
0/100	S_X 55.4 (0.09) S_C* 76.4 (0.25) S_A 81.2 (0.73) I S_X 53.4 (0.13) S_C* 75.2 (0.32) S_A 80.3 (0.70) I	I 73.8 (−0.98) S_A 72.6 (*b*) S_C* 49.1 (−0.12) S_X
11.5/88.5	S_X 54.9 (0.12) S_C* 76.4 (0.29) S_A 81.3 (0.78) I S_X 54.2 (0.12) S_C* 76.0 (0.31) S_A 80.7 (0.71) I	I 74.3 (−0.74) S_A 72.7 (−0.26) S_C* 50.0 (−0.12) S_X
21.8/78.2	S_X 55.5 (0.13) S_C* 76.6 (0.26) S_A 81.6 (0.75) I S_X 54.9 (0.13) S_C* 76.4 (0.29) S_A 81.3 (0.77) I	I 74.2 (−0.98) S_A 72.6 (*b*) S_C* 49.9 (−0.12) S_X
38.9/61.1	S_X 56.5 (0.15) S_C* 76.9 (0.28) S_A 82.0 (0.79) I S_X 55.4 (0.15) S_C* 76.5 (0.29) S_A 81.4 (0.72) I	I 75.1 (−0.72) S_A 73.2 (−0.30) S_C* 51.6 (−0.15) S_X
50.0/50.0	S_X 57.1 (0.13) S_C* 77.1 (0.26) S_A 82.2 (0.76) I S_X 55.7 (0.15) S_C* 76.7 (0.24) S_A 81.6 (0.72) I	I 75.3 (−0.76) S_A 73.4 (−0.20) S_C* 52.2 (−0.14) S_X
59.2/40.8	S_X 57.5 (0.16) S_C* 77.4 (0.29) S_A 82.3 (0.79) I S_X 56.6 (0.16) S_C* 77.0 (0.28) S_A 82.0 (0.74) I	I 75.9 (−0.71) S_A 73.8 (−0.28) S_C* 53.0 (−0.15) S_X
80.9/19.1	S_X 58.8 (0.14) S_C* 77.9 (0.28) S_A 82.6 (0.78) I S_X 58.2 (0.16) S_C* 77.6 (0.31) S_A 82.2 (0.71) I	I 75.8 (−0.71) S_A 74.1 (−0.26) S_C* 53.9 (−0.15) S_X
100/0	S_X 60.4 (0.15) S_C* 78.5 (0.30) S_A 82.9 (0.75) I S_X 59.7 (0.17) S_C* 78.2 (0.33) S_A 82.5 (0.71) I	I 76.4 (−0.68) S_A 74.7 (−0.31) S_C* 55.2 (−0.16) S_X

[a] Data on the first line are from first heating and cooling scans. Data on the second line are from second heating scan. Heating and cooling rates are 10 °C/min. [b] Overlapped peak.

Homopolymerization of (*R*)- and (*S*)-8. The homopolymerizations of (*R*)- and (*S*)-8 are presented in Scheme 2. All polymerizations were carried out at 0 °C in CH_2Cl_2 by a living cationic polymerization technique using $CF_3SO_3H/(CH_3)_2S$ as an initiation system. Previous work in our laboratory[15] and others[16] has shown that the CF_3SO_3H-initiated polymerization of vinyl ethers in the presence of a Lewis base such as $(CH_3)_2S$ gives well-defined polymers with controlled molecular weights and narrow polydispersities. The polymerization mechanism is discussed in detail in previous publications.[10,11,15]

The characterization of poly[(*R*)-8] and poly[(*S*)-8] by gel permeation chromatography (GPC) and differential scanning calorimetry (DSC) is summarized in Tables 1 and 2 respectively. The low polymer yields are the result of the loss of polymer during purification. Relative number-average molecular weights of polymers determined by GPC exhibit a linear dependence on the initial molar ratio of monomer to initiator ($[M]_o/[I]_o$) as shown in Figure 3. All polydispersities are less than 1.23. The $[M]_o/[I]_o$ ratio provides a good control of the polymer molecular weight. All these features demonstrate the typical characteristics of the living polymerization mechanism. The absolute number-average molecular weights were difficult to determine by ^1H NMR spectroscopy from the chain ends of the polymer owing to signal overlap.

The mesomorphic behaviors of poly[(*R*)-8] and poly[(*S*)-8] were investigated by DSC and thermal optical polarized microscopy. Figures 4 and 5 present the DSC thermograms of poly [(*R*)-8] and poly[(*S*)-8] with various degrees of polymerization (DP) respectively. The phase behaviors of the two enantiomeric homopolymers can be compared by superimposing the plots of the dependencies of their thermal transition temperatures as a function of DP (Figure 6). As observed from this figure, the phase behavior of poly[(*R*)-8] is identical to that of poly[(*S*)-8]. The DSC curves of first heating scans are very similar to those of second heating scans except that medium molecular weight polymers (DP = 6.9–8.7) exhibit a small crystalline melting peak on the first heating scan. On the second and subsequent heating scans, all polymers show a S_C* phase followed by a S_A phase which melts into an isotropic phase. In polymers with DP > 7, another higher order smectic phase (S_X) is observed below the S_C* phase. The nature of this S_X phase was not identified. The S_X and S_C* phases are enantiotropic phases since these phases

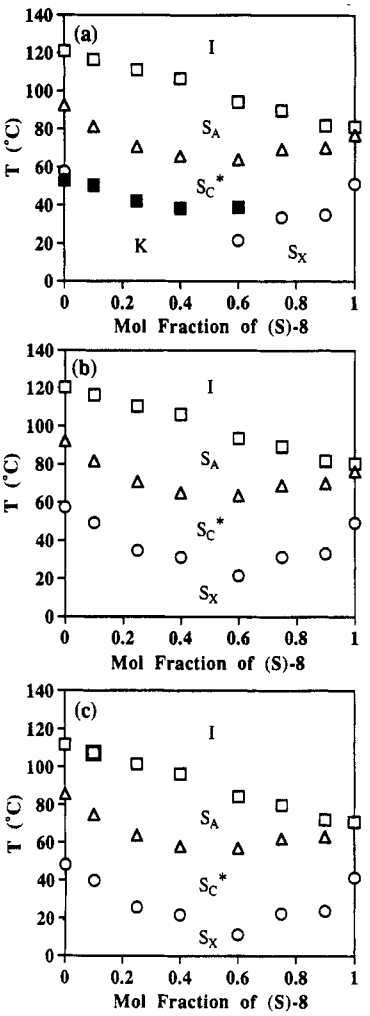

Figure 9. Dependence of phase transition temperatures on the composition of poly[[(*S*)-8]-*co*-[(2*S*,3*S*)-9]].

are also observed in first and subsequent cooling scans. The S_A phase, however, is not observed during the cooling scans. This is most probably due to the thermal instability of the S_A phase whose temperature range is so narrow that the transitions are overlapped with I–S_C* transitions under the relatively high rate of the DSC (20 °C/min). In fact, DSC scans at lower cooling rate (e.g. 10 °C/min) give rise to the very narrow S_A phase in between the I and S_C* phases. A representative optical micrograph of the texture

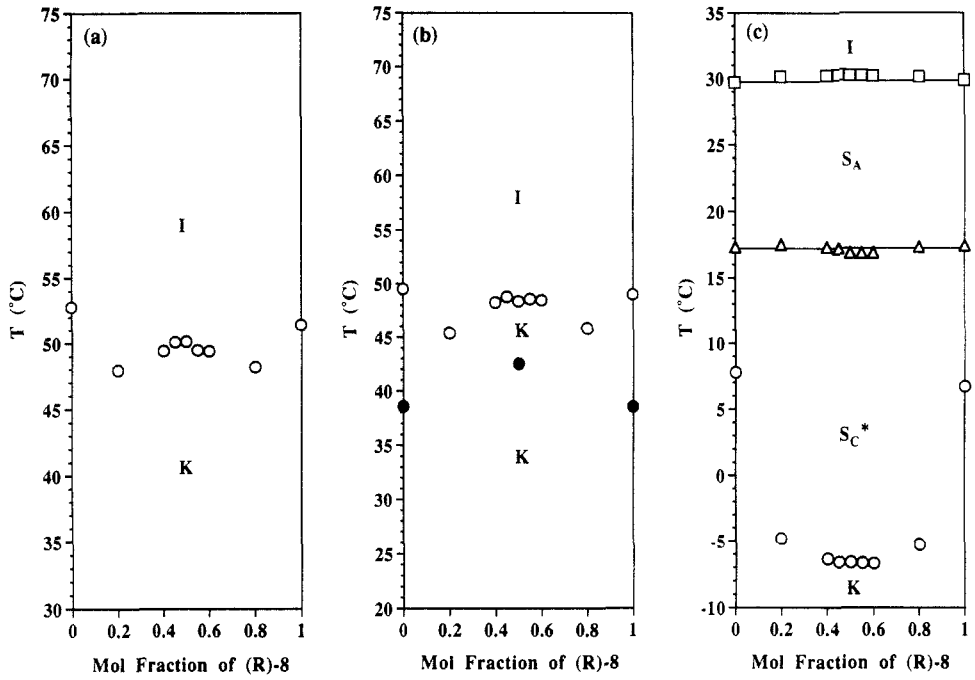

Figure 10. Dependence of phase transition temperatures on the composition of the binary mixtures of (*R*)-8 with (*S*)-8: (a) data from the first heating scans, (b) data from the second heating scans, and (c) data from the first cooling scans.

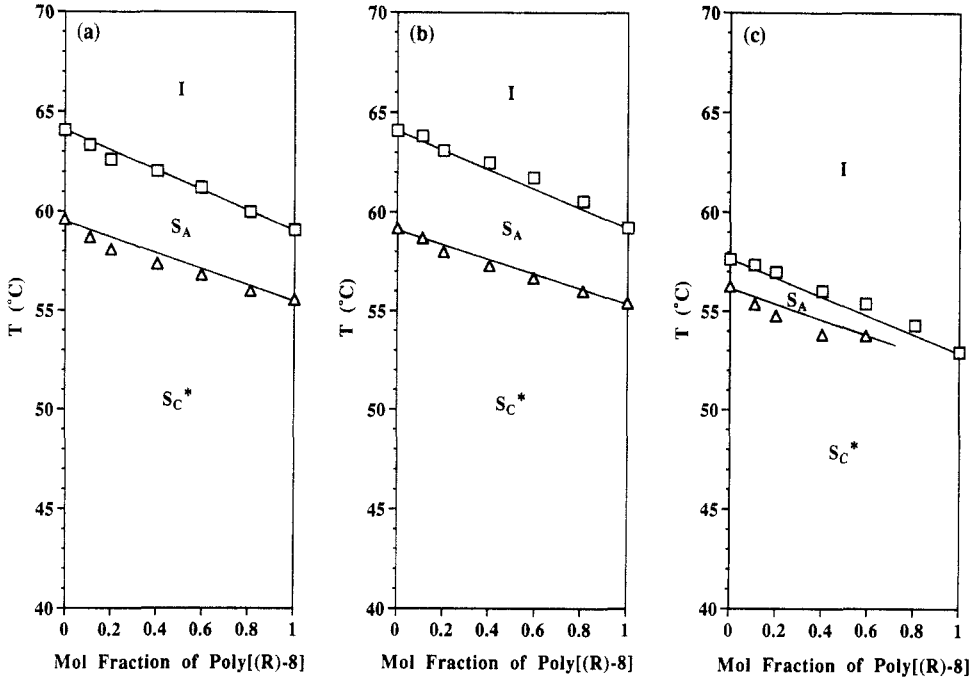

Figure 11. Dependence of phase transition temperatures on the composition of polymer mixture I [poly[(*R*)-8] (DP = 5.7) and poly[(*S*)-8] (DP = 6.1)]: (a) data from the first heating scans, (b) data from the second heating scans, and (c) data from the first cooling scans.

exhibited by the S_A phase of poly[(*S*)-8] (DP = 11.8) is presented in Figure 7.

Since no definitive evidence for the existence of the S_C* phase (e.g. a focal conic texture with equidistant lines) was obtained from the optical microscope analysis, copolymerization experiments between monomer (*S*)-8 and (2*S*,3*S*)-2-fluoro-3-methylpentyl 4′-[[11-(vinyloxy)undecanyl]oxy]biphenyl-4-carboxylate ((2*S*,3*S*)-9), whose homopolymer displays S_A and S_C* phases,[12] were performed to confirm further the phase assignment. On the basis of our previous experience, copolymers derived from two monomers which lead to two homopolymers displaying the same mesophase will show a continuous dependence of their phase transitions on copolymer composition. On the contrary, if the structural units of these two homopolymers are not isomorphic within a particular mesophase, a triple point will occur on the phase diagram.[11b-d,17] Scheme 3 illustrates the copolymerization of (*S*)-8 with (2*S*,3*S*)-9. Attempts were made to synthesize poly[[(*S*)-8)]-*co*-[(2*S*,3*S*)-9]]*X*/*Y* (where *X*/*Y* refers to the mole ratio of the two structural units) with DP = 20. The copolymerization results are summarized in Table 3. The copolymer yields are lower than quantitative due to the polymer losses during the purification process. However, all conversions were quantitative and therefore, the copolymer composition is identical to that of the monomer feed.[10] The DSC traces and the phase diagrams of the copolymers are presented in Figures 8 and 9, respectively. It is clear from these figures that the S_A and S_C* mesophases display a continuous dependence over the

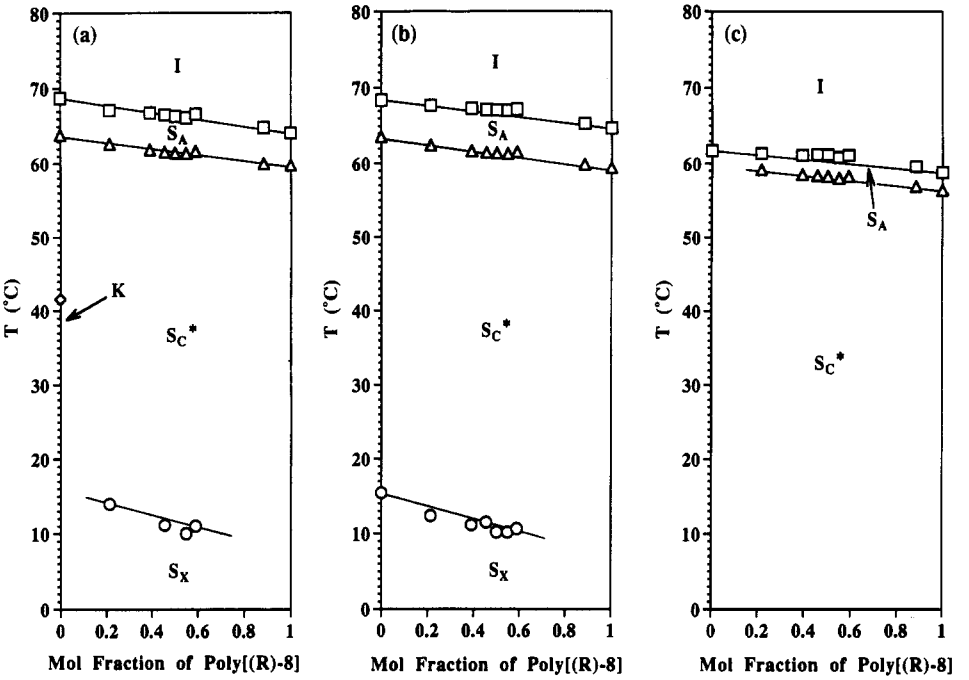

Figure 12. The dependence of phase transition temperatures on the composition of polymer mixture II [poly[(*R*)-8] (DP = 6.7) and poly[(*S*)-8] (DP = 6.9)]: (a) data from the first heating scans, (b) data from the second heating scans, and (c) data from the first cooling scans.

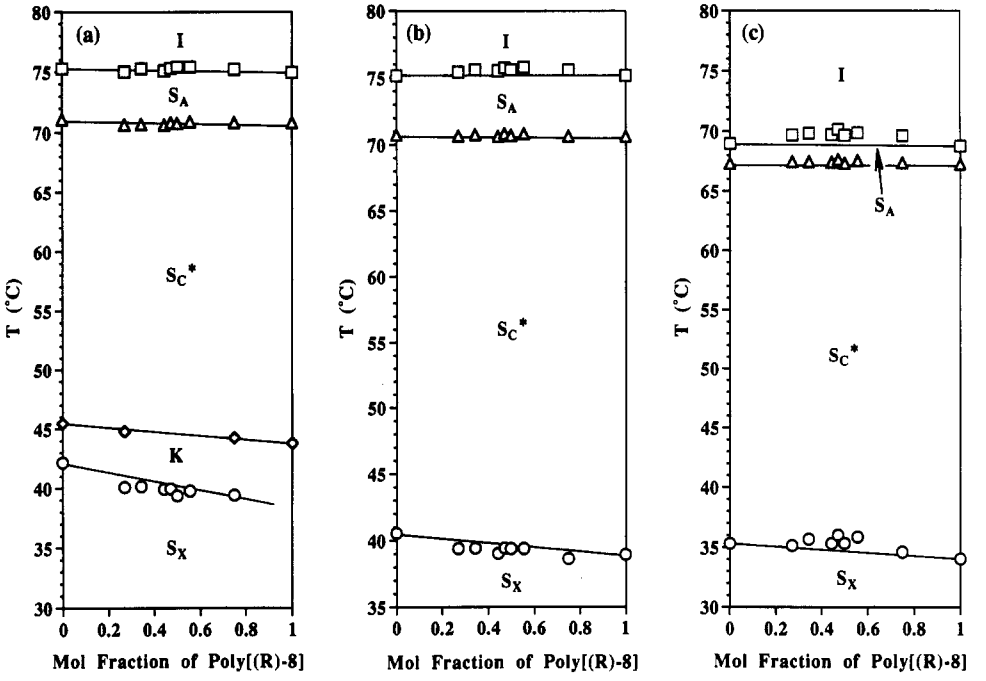

Figure 13. The dependence of phase transition temperatures on the composition of polymer mixture III [poly[(*R*)-8] (DP = 9.6) and poly[(*S*)-8] (DP = 10.1): (a) data from the first heating scans, (b) data from the second heating scans and (c) data from the first cooling scans.

entire composition range, supporting the above phase assignment of poly[(*S*)-8]. It also appears that the two S_X phases of poly[(*S*)-8] and poly[(2*S*,3*S*)-9] are isomorphic.

Miscibility Studies. Monomer (*R*)-8 and monomer (*S*)-8 were mixed in various compositions and the phase behavior of their mixtures was investigated by DSC. Mixtures were prepared by dissolving the two monomers in CH_2Cl_2 followed by evaporation of the solvent under vacuum. Four sets of binary mixtures between poly[(*R*)-8] and poly[(*S*)-8] with different molecular weights were also prepared and their phase behaviors were investigated in the same manner. The molecular weights and polydispersities of the polymers employed in this miscibility study are as follows: (polymer mixture I) poly[(*R*)-8] with DP = 5.7, M_w/M_n = 1.14, and poly[(*S*)-8] with DP = 6.1, M_w/M_n = 1.23; (polymer mixture II) poly[(*R*)-8] with DP = 6.7, M_w/M_n = 1.23, and poly[(*S*)-8] with DP = 6.9, M_w/M_n = 1.21; (polymer mixture III) poly[(*R*)-8] with DP = 9.6, M_w/M_n = 1.16, and poly[(*S*)-8] with DP = 10.1, M_w/M_n = 1.16; (polymer mixture IV) poly[(*R*)-8] with DP = 15.1, M_w/M_n = 1.20, and poly[(*S*)-8] with DP = 14.3, M_w/M_n = 1.19. The thermal transition temperatures and the corresponding enthalpy changes are summarized in Table 4 (for the monomer mixtures) and Tables 5–8 (for the polymer mixtures). The phase diagrams of the monomer mixtures are presented in Figure 10 and the phase diagrams of the polymer mixtures are presented in Figures 11–14.

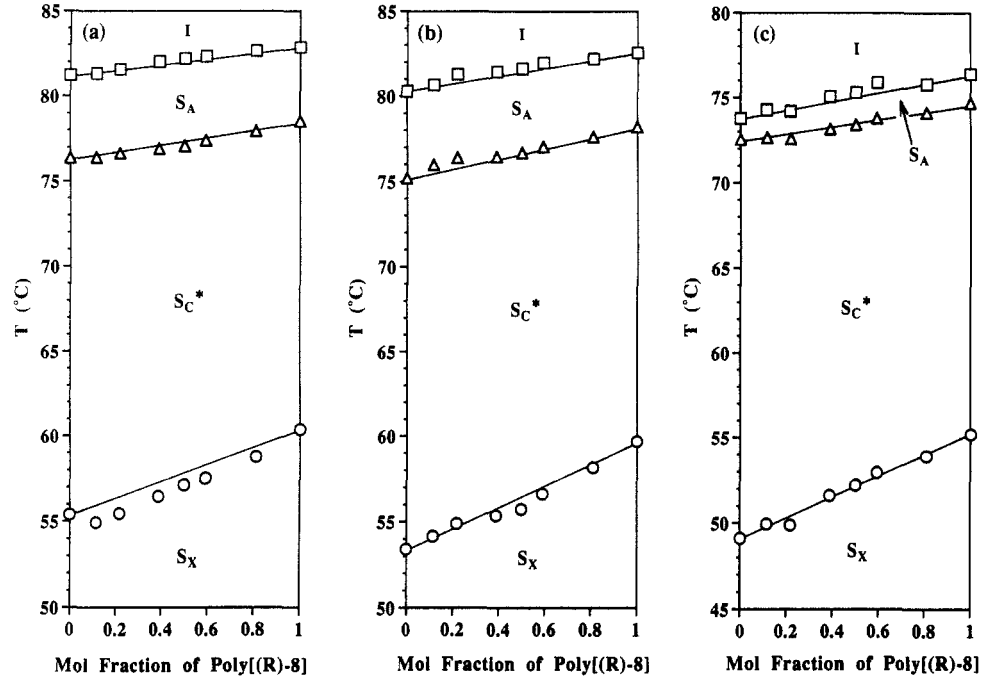

Figure 14. The dependence of phase transition temperatures on the composition of polymer mixture IV [poly(*R*)-8] (DP = 15.1) with poly[(*S*)-8] (DP = 14.3)]: (a) data from the first heating scans, (b) data from the second heating scans, and (c) data from the first cooling scans.

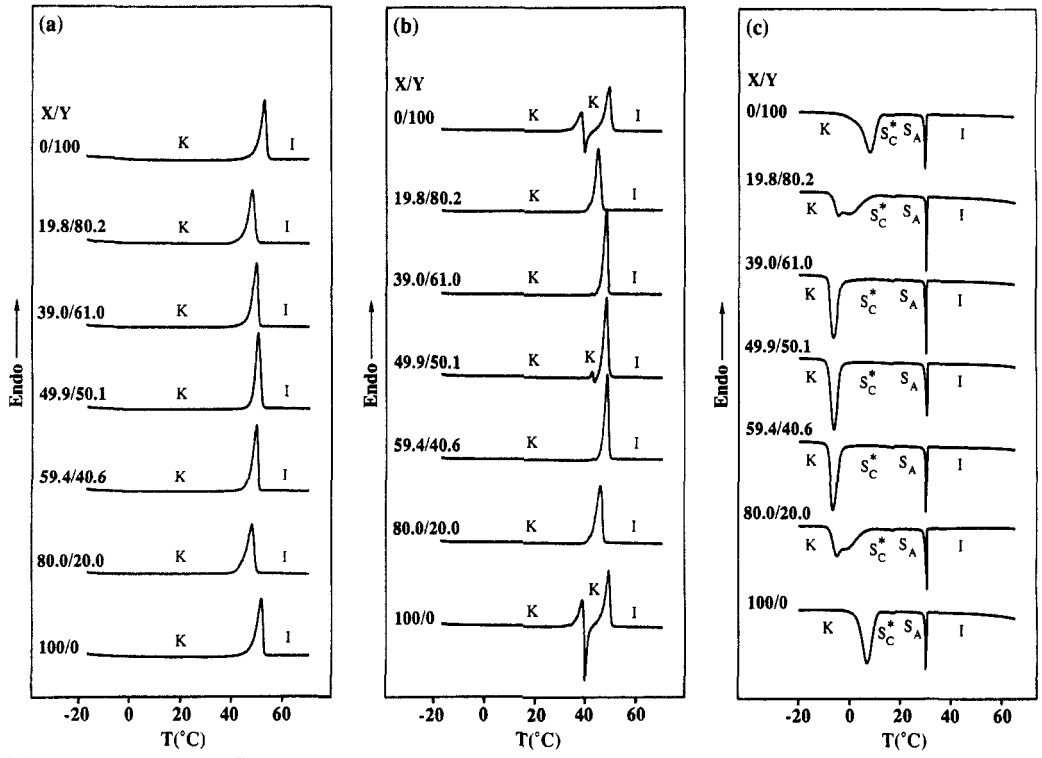

Figure 15. DSC thermograms (10 °C/min) of the binary mixtures of monomer (*R*)-8 (*X*) with monomer (*S*)-8 (*Y*): (a) first heating scans, (b) second heating scans, and (c) first cooling scans.

The DSC thermograms of the monomer mixtures and polymer mixture III are presented in Figures 15 and 16, respectively.

The phase behavior of monomer (*R*)-8 is exactly identical to that of monomer (*S*)-8 and both monomers display monotropic S_A and S_C^* phases and a crystalline phase (Figure 10). When the two monomers were mixed, DSC heating scans showed two eutectic points, while on coolings a large crystalline phase suppression with one eutectic point was observed. On the second and subsequent heating scans, the two pure monomers and a 50/50 monomer mixture showed a crystallization peak. In the S_A and S_C^* phases obtained during the cooling scans, the two enantiomeric structural units of the monomers are miscible and isomorphic over the entire range of compositions. The S_A–I transition temperatures showed an upward curvature, i.e., a positive deviation (0.4 °C) from the linear dependence predicted by the Schröder–van Laar equation for an ideal solution,[18,19] demonstrating the presence of the chiral molecular recognition between the two enantiomeric structural units. On the contrary, the S_C^*–S_A transition temperatures showed negative deviations (−0.5 °C) from the theoretical values. These two contrasting behaviors shown by the S_A–I and S_C^*–S_A transitions are identical to

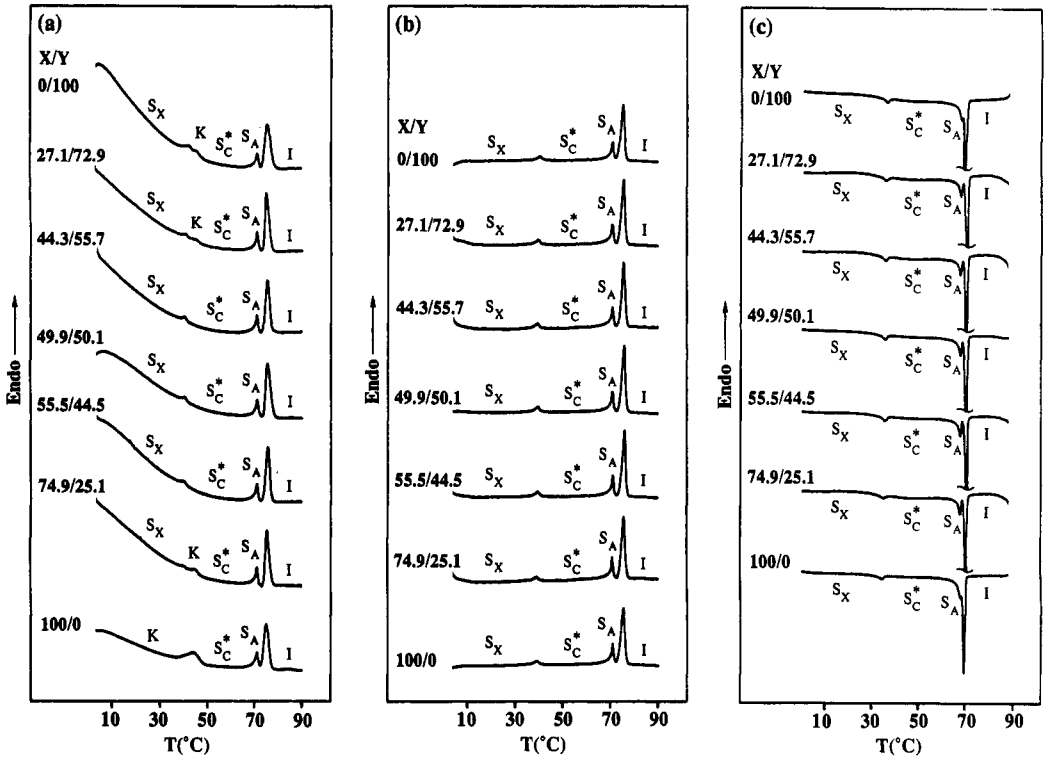

Figure 16. DSC thermograms (10 °C/min) of polymer mixture III [poly[(*R*)-8] (DP = 9.6) and poly[(*S*)-8] (DP = 10.1)]: (a) first heating scans, (b) second heating scans, and (c) first cooling scans.

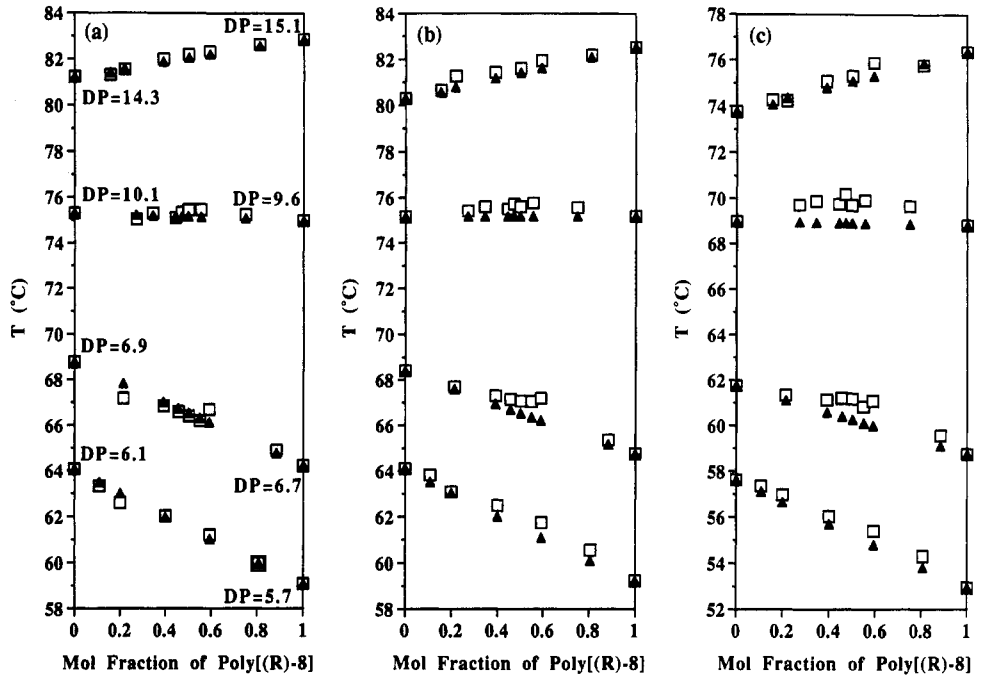

Figure 17. Dependence of the S_A–I transition temperatures from experimental data (open symbols) and from the Schröder–van Laar equation (closed symbols) on the composition of the binary mixtures of poly[(*R*)-8] with poly[(*S*)-8]: (a) data from the first heating scans, (b) data from the second heating scans, and (c) data from the first cooling scans.

those reported in a previous publication on the phase behavior of two diastereomeric liquid crystalline monomer pairs.[12]

In the four sets of polymer mixtures with different molecular weights, the two enantiomeric structural units derived from the two monomers are also miscible and isomorphic in all mesophases across the full composition range. The S_A–I transitions always show an upward curvature on the second heating scans and the first cooling scans.

In order to compare the S_A–I transition temperatures quantitatively, all the S_A–I transition temperatures obtained from the four sets of polymer mixtures are summarized in Figure 17 (open symbols) together with the corresponding theoretical values calculated from the Schröder–van Laar equation (closed symbols). Since the enthalpy changes associated with the S_A–I transitions are almost identical for the two enantiomeric polymers possessing similar molecular weights, the Schröder–van Laar equation predicts for an ideal solution like mixture a linear dependence of the S_A–I transition temperatures on composition in all cases. Consequently, the upward curvatures shown in Figure 17 are indicating the presence of chiral recognition in all the polymer mixtures as well

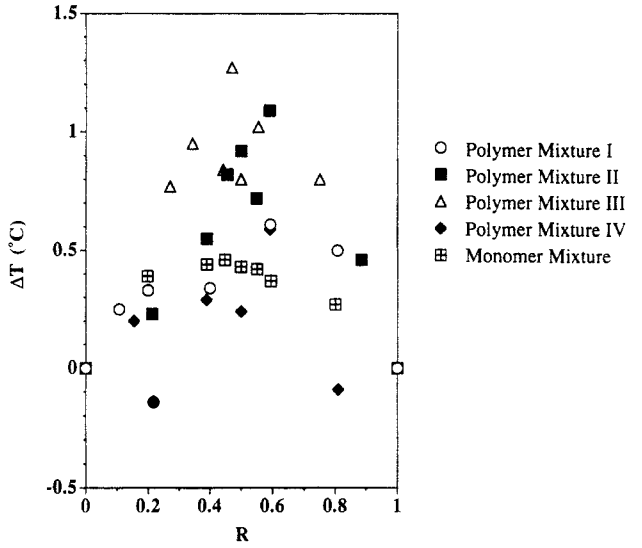

Figure 18. Deviation of the S_A–I transition temperatures collected during the first cooling scans from the theoretical ideal values (ΔT) *versus* composition.

as in the monomer mixtures. Figure 18 displays the deviation (ΔT) of the S_A–I transition temperatures collected during the first cooling scans from the theoretical values *versus* mixture compositions. The data obtained from the monomer mixtures are also plotted in this figure. The reason for the fluctuation of data points which can be seen in this figure is not clear. Regardless of the fluctuation of the data points, the following trends can be easily observed from Figure 18. With increasing the molecular weight i.e., on going from the monomer mixtures to the polymer mixtures I, II, and III, ΔT increases in the same order to reach a positive deviation of 1.3 °C from the theoretical ideal value. The polymer mixtures IV (polymer mixtures with the largest molecular weight) show, on the contrary, a smaller ΔT deviation than that of the monomer mixtures. These trends clearly suggest that there is an optimum molecular weight which favors the largest chiral molecular recognition. To a certain amount of molecular weight, the polymer backbone "effect" enhances the chiral molecular recognition effect between the two enantiomeric side chain structural units through a cooperative effect.[20,21] However, when the molecular weight of the polymer exceeds a critical value, the polymer backbone decreases the heterochiral interaction between the enantiomeric side groups, resulting in the cancellation of chiral molecular recognition. The trend of the influence of molecular weight on the ΔT deviation observed here suggests that the equilibrium constant of the heterochiral recognition process is molecular weight dependent. The dependence of the ΔT deviation observed in this case resembles that of the trend observed for the dependence of the equilibrium constant of interpolymeric electron donor–acceptor complexes on molecular weight.[21b]

With respect to the S_C*–S_A and S_X–S_C* transitions of the polymer mixtures, it seems that the dependence of transition temperatures on the composition is not very clear. In Figures 11 and 14a and S_C*–S_A transitions show a downward curvature, while in Figures 12 and 13 they look insensitive to the composition. This is probably due to the fact that the S_C*–S_A transitions are in close proximity of the S_A–I transitions, and they are partially overlapped. This can cause the inaccurate determination of the temperatures of the S_C*–S_A transitions whose peak are much smaller than those of the S_A–I transitions.

Copolymerization of (*R*)- and (*S*)-8. Copolymerization of (*R*)-8 with (*S*)-8 was performed to cover the

Table 9. Cationic Copolymerization of (*R*)-8 with (*S*)-8 and Characterization of the Resulting Polymers[a]

[(*R*)-8]/[(*S*)-8] (mol)/(mol)	polymer yield (%)	$M_n \times 10^{-3}$	M_w/M_n	DP	phase transitions (°C) and corresponding enthalpy changes (kcal/mru)[b]	
					heating	cooling
0/100	76.2	4.99	1.16	10.1	S_X 42.2 (0.21) K 45.5 (*a*) S_C* 71.1 (0.17) S_A 75.3 (0.80) I	I 69.0 (–1.00) S_A 67.3 (*c*) S_C* 35.9 (–0.07) S_X
					S_{X1} 40.6 (0.08) S_C* 70.7 (0.28) S_A 75.2 (0.71) I	
20/80	79.3	5.17	1.15	10.6	S_X 44.7 (0.10) S_C* 72.9 (0.27) S_A 77.7 (0.86) I	I 70.7 (–1.07) S_A 69.1 (*c*) S_C* 39.5 (–0.07) S_X
					S_X 44.1 (0.10) S_C* 72.8 (0.25) S_A 77.4 (0.82) I	
40/60	64.3	5.00	1.16	10.3	S_X 36.6 (0.05) S_C* 70.1 (0.29) S_A 75.8 (0.79) I	I 69.0 (–0.75) S_A 66.5 (–0.28) S_C* 31.5 (–0.07) S_X
					S_X 35.4 (0.08) S_C* 70.1 (0.29) S_A 75.8 (0.78) I	
50/50	83.8	5.18	1.15	10.6	S_X 43.4 (0.10) S_C* 72.4 (0.26) S_A 77.3 (0.85) I	I 70.4 (–0.84) S_A 68.6 (–0.31) S_C[c] 38.9 (–0.12) S_X
					S_X 43.0 (0.13) S_C* 72.4 (0.27) S_A 77.2 (0.90) I	
60/40	81.7	5.20	1.15	10.7	S_X 42.1 (0.09) S_C* 72.0 (0.25) S_A 76.8 (0.84) I	I 70.2 (–0.75) S_A 68.4 (–0.28) S_C* 37.7 (–0.10) S_X
					S_X 41.5 (0.10) S_C* 71.8 (0.26) S_A 76.5 (0.82) I	
80/20	78.8	4.96	1.17	10.2	S_X 39.3 (0.06) S_C* 70.6 (0.30) S_A 76.0 (0.81) I	I 68.3 (–1.12) S_C* 33.0 (–0.07) S_X
					S_X 38.2 (0.10) S_C* 70.5 (0.32) S_A 75.6 (0.86) I	
100/0	91.0	4.98	1.12	10.2	K 37.3 (0.25) S_X 40.0 (*c*) S_C* 72.6 (0.29) S_A 77.0 (0.78) I	I 70.2 (–0.97) S_C* 34.9 (–0.06) S_X
					S_X 39.3 (0.08) S_C* 72.4 (0.29) S_A 76.5 (0.79) I	

[a] Polymerization temperature, 0 °C; polymerization solvent, methylene chloride; $[M]_o = [(R)\text{-}8] + [(S)\text{-}8] = 0.224$; $[M]_o/[I]_o = 16$; $[Me_2S]_o/[I]_o = 10$; polymerization time, 1 h. [b] Heating and cooling rates are 10 °C/min. Data on the first line are from first heating and cooling scans. Data on the second line are from second heating scan. [c] Overlapped peak.

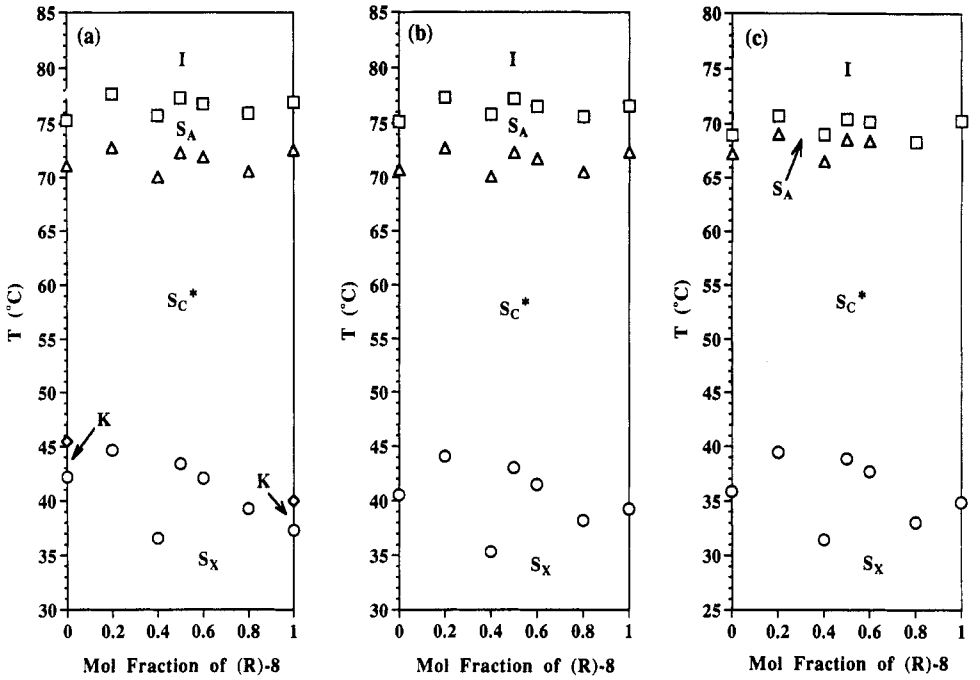

Figure 19. Dependence of the phase transition temperatures on the composition of poly[(*R*)-8-*co*-(*S*)-8] (DP = 10.1–10.7): (a) data from the first heating scans, (b) data from the second heating scans, and (c) data from the first cooling scans.

entire range of composition. Attempts were made to synthesize poly[[(*R*)-8]-*co*-[(*S*)-8]] with DP = 16. Since the transition temperatures of polymers are strongly dependent on their molecular weights, it is essential to synthesize polymers having identical molecular weights in order to compare their transition temperatures. This can be achieved only by a living polymerization. The copolymerization results are listed in Table 9. The yields reported in Table 9 are lower than quantitative due to the polymer losses during the purification process. However, all conversions were quantitative and therefore, the copolymer composition is identical to that of the monomer feed.[10] The average degrees of polymerization determined by GPC are 10–11.

The thermal transition temperatures determined by DSC are listed in Table 9 and are plotted against copolymer composition in Figure 19. The copolymers poly[[(*R*)-8]-*co*-[(*S*)-8]] exhibit the same phase behavior as their parent homopolymers over the entire range of compositions. Although the molecular weights of these copolymers are rather well controlled, the fluctuation of the experimental data points is large and therefore, no clear trends are observed for phase transitions.

Conclusions

In the previous publication of this series, we investigated the heterochiral molecular recognition in molecular and macromolecular pairs of diastereomeric liquid crystals based on (2*R*,3*S*)- and (2*S*,3*S*)-2-fluoro-3-methylpentyl 4′-[[11-(vinyloxy)undecanyl]oxy]biphenyl-4-carboxylate (**9**) diastereomers. It was observed that chiral recognition was present in the S_A phase of monomer mixtures; however, it was canceled in polymer mixtures and in copolymers.[12] The current study provides the first example of heterochiral molecular recognition in enantiomeric pairs of low molar mass and side-chain liquid crystalline polymers. It also presents the first experiments that demonstrate a dependence of heterochiral molecular recognition on polymer molecular weight. In the present case as in the previously reported one,[12] heterochiral molecular recognition was observed only in the untilted S_A phase. These results are in agreement with all other data available in the literature on low molar mass liquid crystals.[1a,5,7,8] On the other hand, no clear relationship between transition temperatures on composition could be obtained for copolymers. This is mostly due to the very low deviation of the transition temperature from ideal values observed for this system. This requires experiments with a more accurate polymerization technique or a pair of enantiomers which provides a larger deviation of the transition temperature as a consequence of the heterochiral recognition process.

Acknowledgment. Financial support by the Office of Naval Research and Asahi Chemical Industry Co., Ltd., Japan is gratefully acknowledged.

References and Notes

(1) (a) Jacques, J.; Collet, A.; Wilen, S. H. *Enantiomers, Racemates and Resolutions*; Krieger Publishing Co.: Malabar, 1991. (b) Pirkle, W. H.; Pochapsky, T. C. *Chem. Rev.* **1989**, *89*, 347. (c) Walba, D. M.; Slater, S. C.; Thurmes, W. N.; Clark, N. A.; Handschy, M. A.; Supon, F. *J. Am. Chem. Soc.* **1986**, *108*, 5210.

(2) (a) Arnett, E. M.; Harvey, N. G.; Rose, P. L. *Acc. Chem. Res.* **1989**, *22*, 131. (b) Rose, P. L.; Harvey, N. G.; Arnett, E. M. In *Advances in Physical Organic Chemistry* Bethell, D., Ed.; Academic Press: New York, 1993; Vol. 28, p 45. (c) Arnett, E. M.; Thompson, O. *J. Am. Chem. Soc.* **1981**, *103*, 968. (d) Harvey, N. G.; Rose, P. L.; Mirajovsky, D.; Arnett, E. M. *J. Am. Chem. Soc.* **1990**, *112*, 3547. (e) Arnett, E. M.; Gold, J. M. *J. Am. Chem. Soc.* **1982**, *104*, 636.

(3) (a) Harvey, N.; Rose, P.; Porter, N. A.; Huff, J. B.; Arnett, E. M. *J. Am. Chem. Soc.* **1988**, *110*, 4395. (b) Heath, J. G.; Arnett, E. M. *J. Am. Chem. Soc.* **1992**, *114*, 4500.

(4) For representative reviews on SC* liquid crystals, see: (a) Goodby, J. W. *Science* **1986**, *231*, 350. (b) Goodby, J. W. *J. Mater. Chem.* **1991**, *1*, 307. (c) Goodby, J. W., Ed. *Ferroelectric Liquid Crystals. Principles, Properties and Applications*; Gordon and Breach Science Publishers: Philadelphia, 1991. (d) LeBarny, P.; Dubois, J. C. In *Side Chain Liquid Crystal Polymers*; McArdle, C. B., Ed.; Chapman and Hall: New York, 1989; p 130. (e) Escher, C.; Wingen, R. *Adv. Mater.* **1992**, *4*, 189.

(5) (a) Leclercq, M.; Billard, J.; Jacques, J. *Mol. Cryst. Liq. Cryst.* **1969**, *8*, 367. (b) Bahr, C. H.; Heppke, G.; Sabaschus, B. *Ferroelectrics* **1988**, *84*, 103. (c) Bahr, C. H.; Heppke, G.; Sabaschus, B. *Liq. Cryst.* **1991**, *9*, 31.

(6) (a) Yamada, Y.; Mori, K.; Yamamoto, N.; Hayashi, H.; Nakamura, K.; Yamawaki, M.; Orihara, H.; Ishibashi, Y. *Jpn. J. Appl. Phys.* **1989**, *28*, L1606. (b) Takezoe, H.; Lee, J.; Chandani, A. D. L.; Gorecka, E.; Ouchi, Y.; Fukuda, A.; Terashima, K.; Furukawa, K. *Ferroelectrics* **1991**, *114*, 187. (c) Takezoe, H.; Fukuda, A.; Ikeda, A.; Takanishi, Y.; Umemoto, T.; Watanabe, J.; Iwane, H.; Hara, M.; Itoh, K. *Ferroelectrics* **1991**, *122*, 167. (d) Goodby, J. W.; Chin, E. *Liq. Cryst.* **1988**, *3*, 1245. (e) Goodby, J. W.; Patel, J. S.; Chin, E. *J. Mater. Chem.* **1992**, *2*, 197. (f) Heppke, G.; Lötzsch, D.; Demus, D.; Diele, S.; Jahn, K.; Zaschke, H. *Mol. Cryst. Liq. Cryst.* **1991**, *208*, 9.

(7) (a) Goodby, J. W.; Waugh, M. A.; Stein, S. M.; Chin, E.; Pindak, R.; Patel, J. S. *J. Am. Chem. Soc.* **1989**, *111*, 8119. (b) Slaney, A. J.; Goodby, J. W. *Liq. Cryst.* **1991**, *9*, 849. (c) Goodby, J. W.; Nishiyama, I.; Slaney, A. J.; Booth, C. J.; Toyne, K. J. *Liq. Cryst.* **1993**, *14*, 37. (d) Nguyen, H. T.; Twieg, R. J.; Nabor, M. F.; Isaert, N.; Destrade, C. *Ferroelectrics* **1991**, *121*, 187. (e) Navailles, L.; Nguyen, H. T.; Barois, P.; Destrade, C.; Isaert, N. *Liq. Cryst.* **1993**, *15*, 479.

(8) (a) Levelut, A. M.; Germain, C.; Keller, P.; Liebert, L.; Billard, J. *J. Phys., Paris* **1983**, *44*, 623. (b) Keller, P. *Mol. Cryst. Liq. Cryst. Lett.* **1984**, *102*. 295. (c) Billard, J.; Dahlgren, A.; Flatischler, K.; Lagerwall, S. T.; Otterholm, B. J. *Phys., Paris* **1985**, *46*, 1241. (d) Heppke, G.; Kleineberg, P.; Lötzsch, D. *Liq. Cryst.* **1993**, *14*, 67.

(9) Lien, S. C.; Huang, C. C.; Goodby, J. W. *Phys. Rev. A* **1984**, *29*, 1371.

(10) For a brief review on the molecular engineering of side chain LCP by living cationic polymerization see: Percec, V.; Tomazos, D. *Adv. Mater.* **1992**, *4*, 548.

(11) (a) Percec, V.; Zheng, Q.; Lee, M. *J. Mater. Chem.* **1991**, *1*, 611. (b) Percec, V.; Zheng, Q.; Lee, M. *J. Mater. Chem.* **1991**, *1*, 1015. (c) Percec, V.; Zheng, Q. *J. Mater. Chem.* **1992**, *2*, 475. (d) Percec, V.; Zheng, Q. *J. Mater. Chem.* **1992**, *2*, 1041.

(12) Percec, V.; Oda, H.; Rinaldi, P. L.; Hensley, D. R. *Macromolecules* **1994**, *27*, 12.

(13) Fu, S. J.; Birnbaum, S. M.; Greenstein, J. P. *J. Am. Chem. Soc.* **1954**, *76*, 6054.

(14) Booth, C. J.; Goodby, J. W.; Hardy, J. P.; Lettington, O. C.; Toyne, K. J. *J. Mater. Chem.* **1993**, *3*, 821.

(15) (a) Percec, V.; Lee, M.; Jonsson, H. *J. Polym. Sci.: Part A: Polym. Chem.* **1991**, *29*, 327. (b) Percec, V.; Lee, M. *Macromolecules* **1991**, *24*, 1017. (c) Percec, V.; Lee, M.; Rinaldi, P.; Litman, V. E. *J. Polym. Sci.: Part A: Polym. Chem.* **1992**, *30*, 1213.

(16) (a) Cho, C. G.; Feit, B. A.; Webster, O. W. *Macromolecules* **1990**, *23*, 1918. (b) Cho, C. G.; Feit, B. A.; Webster, O. W. *Macromolecules* **1992**, *25*, 2081. (c) Lin, C. H.; Matyjaszewski, K. *Polym. Prepr., Am. Chem. Soc. Div. Polym. Chem.* **1990**, *31*, 599.

(17) (a) Percec, V.; Lee, M. *Polymer* **1991**, *32*, 2862. (b) Percec, V.; Lee, M. *Polymer Bull.* **1991**, *25*, 131. (c) Percec, V.; Lee, M. *Macromolecules* **1991**, *24*, 4963. (d) Percec, V.; Lee, M. *J. Mater. Chem.* **1991**, *1*, 1007. (e) Percec, V.; Lee, M. *J. Mater. Chem.* **1992**, *2*, 617.

(18) (a) Van Hecke, G. R. *J. Phys. Chem.* **1979**, *83*, 2344. (b) Achard, M. F.; Mauzac, M.; Richard, H.; Sigaud, G.; Hardouin, F. *Eur. Polym. J.* **1989**, *25*, 593.

(19) (a) Percec, V.; Lee, M. *J. Mater. Chem.* **1991**, *1*, 1007. (b) Percec, V.; Lee, M.; Zheng, Q. *Liq. Cryst.* **1992**, *12*, 715. (c) Percec, V.; Johansson, G. *J. Mater. Chem.* **1993**, *3*, 83.

(20) (a) Ciardelli, F.; Salvadori, P. *Pure Appl. Chem.* **1985**, *57*, 931. (b) Selegny, E., Ed. *Optically Active Polymers*; D. Reidel Publishing Co.: Dordrecht, The Netherlands, 1979. (c) Matsuzaki, K.; Watanabe, T. *Makromol. Chem.* **1971**, *146*, 109.

(21) (a) Pugh, C.; Rodriguez-Parada, J.; Percec, V. *J. Polym. Sci.: Part A: Polym. Chem.* **1986**, *24*, 747. (b) Percec, V.; Schild, H. G.; Rodriguez-Parada, J. M.; Pugh, C. *J. Polym. Sci.: Part A: Polym. Chem.* **1988**, *26*, 935.